

CHALMERS



Plucked Instrument Strings:

A Combined Frequency - Time Domain Wave Approach to
Investigate Longitudinal Forces at the Bridge Support

Master's Thesis in the Master's programme in Sound and Vibration

MATTHEW DAVID TUTTLE

Department of Civil and Environmental Engineering
Division of Division of Applied Acoustics
Vibroacoustics Group and Room Acoustics Group
CHALMERS UNIVERSITY OF TECHNOLOGY
Göteborg, Sweden 2007

Master's Thesis 2007:71

MASTER'S THESIS 2007:71

Plucked Instrument Strings:

A Combined Frequency - Time Domain Wave Approach to
Investigate Longitudinal Forces at the Bridge Support

Matthew David Tuttle

Department of Civil and Environmental Engineering
Division of Applied Acoustics
Room Acoustics Group and Vibroacoustics Group
CHALMERS UNIVERSITY OF TECHNOLOGY
Göteborg, Sweden 2007

Plucked Instrument Strings:
A Combined Frequency - Time Domain Wave Approach to Investigate Longitudi-
nal Forces at the Bridge Support

© Matthew David Tuttle, 2007

Master's Thesis 2007:71

Department of Civil and Environmental Engineering
Division of Applied Acoustics
Room Acoustics Group and Vibroacoustics Group
Chalmers University of Technology
SE-41296 Göteborg
Sweden

Tel. +46-(0)31 772 1000

Reproservice / Department of Civil and Environmental Engineering
Göteborg, Sweden 2007

Plucked Instrument Strings:

A Combined Frequency - Time Domain Wave Approach to Investigate Longitudinal Forces at the Bridge Support

Master's Thesis in the Master's programme in Sound and Vibration

Matthew David Tuttle

Department of Civil and Environmental Engineering

Division of Applied Acoustics

Room Acoustics Group and Vibroacoustics Group

Chalmers University of Technology

Abstract

The transverse wave motion of strings in musical instruments is the predominant influence on the instrument's radiated sound. However, longitudinal waves, generated by their coupling to transverse waves, can also give a noticeable contribution. The main goal of this thesis is to develop a computer model to help investigate and understand how longitudinal waves are generated and then juxtapose the obtained information with measurements made on a unique single stringed instrument. The model uses a frequency domain transverse wave approach followed by a time domain calculation of the transverse to longitudinal wave coupling. The instrument apparatus is made of wood and contains one single string stretched between two bridge points. The string and its base are completely separate from the plectrum, jack and key. This prevents measuring vibrations other than those of the string's. A supplementary goal of the thesis is investigating plectrum, jack and string interaction during excitation.

The transverse wave model appears to be accurate in comparison to measurements made on the measurement apparatus. Unfortunately, the same statement cannot be made about the longitudinal wave model because of a lack of good measurement data. Observations of transversal to longitudinal wave coupling and subsequent longitudinal wave forces are made by testing different inputs into the model.

Acknowledgements

I would foremost like to thank my adviser, Matthias Scholz, for his patience, his pedagogical advice, his genuine interest in all the work we performed and his ability to take one idea and create twenty from it. Next, I would like to thank the generosity and knowledge given by everyone at the Department of Applied Acoustics at Chalmers. I never once felt alone when I had a question regarding anything.

It is also important to give thanks to the talented Gregor Bergmann at Organ Workshop Ahrend in Leer, Germany, who built the instrument apparatus (Appendix A) used in our measurements.

I would personally like to thank Hannes Bonhoff, who was the conductor for our group of master's students 2004. He helped create what will probably be the greatest year of my life. I also give him credit for introducing me to climbing. I also thank all of my friends and peers whom I was privileged to meet while in Göteborg. I could not have learned as much with as much enjoyment and ease if it were not for them.

Ultimately, I thank my parents and family for always supporting me and trusting my decisions. I would not be where I am today if it were not for their genetics, advice, finances and love.

Contents

Abstract	iii
Acknowledgements	v
Contents	vi
1 Introduction and Motivation	1
2 Transverse Vibration Model	5
2.1 Method	5
2.2 Formulation	6
2.3 Boundary Conditions	10
2.4 Results	11
3 Adaptation of Input Force	17
4 Longitudinal Wave Model	25
4.1 Formulation	25
4.2 Model	27

5	Forces at the Bridge	29
5.1	Formulation	29
5.2	Results	30
6	Conclusions	37
A	Measurement Apparatus	41
B	MATLAB Code	43
B.1	Wavenumber and Coefficient Calculations	43
B.2	Input Force	50
B.3	Bridge Acceleration	51
B.4	Longitudinal Displacement - Part 1	52
B.5	Longitudinal Displacement - Part 2	61
B.6	Longitudinal Bridge Force	63
	Notations	65

Chapter 1

Introduction and Motivation

Coupling of transverse to longitudinal string vibrations has been an interest of many researchers in musical acoustics, and the question of whether longitudinal forces acting on the bridge of musical instruments have significant influence on the radiated sound came to my attention during the master's thesis work of Ben Henley.

Henley's main aim was investigating sound radiation in the time domain of a plucked string musical instrument called a virginal [7]. His initial concept was to scan a plane around the instrument to show effects of spatially varying sound source characteristics, i.e. show that the regions of major sound radiation temporarily varied over the instrument's surface. In order to conduct such an experiment, it is necessary to excite the string in a repeatable manner so each excitation is the same as the previous. Since the interaction between string and key is highly non-linear and partially chaotic, it is not possible to excite the string in a repeatable manner. To obtain this needed repeatability, it was decided to replace the string's forces at the bridge of the instrument by a shaker input with a transient signal similar to that of a plucked string.

Finding a transient signal, such as resulting forces at an instrument's bridge due to a vibrating string, can be accomplished using an LMS algorithm technique similar to a method developed by Wolfgang Kropp and Krister Larsson and then later tested by Eskil Lindberg [10]. The goal in Kropp and Larsson's work was to develop an algorithm allowing them to estimate forces at locations on a vibrating structure that are not able to be measured directly for some situational reason.

Henley borrowed this idea and applied it to his work when he found difficulty mea-

asuring the string forces at the virginal's bridges. He presumed that once string input forces at the bridges were identified using the LMS algorithm technique, shakers could then replace the string and apply the same forces to the instrument body as the excited string and do so in a repeatable manner.

In Henley's experiments, once the force function had been identified and applied to the virginal with shakers, the shaker excitation gave an audible deviation from the virginal sound excited by the string. The entire reproduction seemed to lack something at higher frequencies. A possible reason for the deviation was only the forces induced vertically at both bridges had been taken into account. The vertical forces at the bridges are likely the dominating means of energy transmission between string and soundboard, however, it has been shown by some authors that horizontal forces are of importance in pianos [6],[1] and can very well excite the soundboard, contributing to the sound radiation.

Though importances of longitudinal string forces on piano's bridges have been previously published, a virginal is only slightly similar to a piano. Both are stringed instruments and contain large initial transverse displacements, though a virginal's excitation is due to a pluck whereas a piano is excited with a hammer strike. The geometries, the constructing materials and the pre-stress of the instruments are also general differences. The motivation of this thesis is to observe whether longitudinal forces play a significant role in the sound production of a virginal using mixed frequency and time domain techniques to model the transverse and ultimately longitudinal wave forces at the instrument's bridges.

One such paper that presents a model to show the presence and generation of longitudinal waves is Baláz Bank and László Sujbert's "Generation of longitudinal vibrations in piano strings: From physics to sound synthesis" [2]. Their paper describes a modal model to predict the prominent components of longitudinal vibration as a function of transverse modal frequencies.

The present paper is largely based on Bank and Sujbert's developed model for transverse to longitudinal wave coupling. Similarly, the model presented here assumes only one plane of transverse vibrations, the coupling of transverse to longitudinal waves is unidirectional, i.e. longitudinal to transverse coupling is neglected, and the level of transverse to longitudinal wave coupling is dependent on the magnitude of the transverse vibration according to a square law.

The main differences between the model presented in this paper and the one developed by Bank and Sujbert are how the transverse waves are generated and modeled. Unlike modal models, like those used by Bank and Sujbert, the present model

allows for all possible transverse frequencies and will only be frequency limited due to the computational resolution. All modes and effects from dispersion will be numerically computed and determined by the physical properties and governing equations of motion for a string.

The present paper is divided into four parts. Chapter 2 presents the frequency domain, transverse wave model and shows comparisons of the acceleration measured at the bridge of the measurement apparatus (see Appendix A) with the acceleration output of the simulated model. Chapter 3 explains the importance and difficulties of modeling the excitation input force. Chapter 3 also discusses methods to measure and understand the plectrum and jack interaction during excitation. Chapter 4 explains how longitudinal waves are theoretically developed and modeled. Chapter 5 shows how forces at the bridge are computed and investigates the generation of longitudinal forces at a stringed instrument's bridge. Concluding remarks are then given in Chapter 6.

Chapter 2

Transverse Vibration Model

2.1 Method

There are a few different common approaches used to model the transverse vibrations of a string. Three of the popular approaches are:

- A modal model, like that developed by Morse [11], which represents the motion of a string using a finite series of modal shapes (standing waves). This method is computationally light but makes strict assumptions about the behavior of the string. Bank and Sujbert use this method in their transverse to longitudinal wave coupling synthesis model.
- A waveguide model, which uses time domain bi-directional delay units, scattering junctions, and digital filters to represent the wave motion, dispersion, and losses of a vibrating string. This computationally light method is used extensively by Smith III and Duyne [5] in sound synthesis but is rarely used to study physics.
- A finite difference method model, which is an energy conservation, physical, state space model based on ideal string equations. Chaigne [3] developed models based on this finite difference approach and has been used by Hiller and Ruiz [8]. This method can require a large computational load but it can also be very adaptable to the physics it describes.

The present model to compute the vertical transverse vibrations of a string is a frequency domain wave approach with the assumption that the string acts as a

thin beam under tension. The wave approach estimates the transverse vibrations of the string by evaluating the propagating bending waves and the corresponding near-fields within the string.

2.2 Formulation

The equation of motion, in one-dimension, of a string or beam in tension can be described by the following equation:

$$B \frac{\partial^4 \eta(x, t)}{\partial x^4} - T \frac{\partial^2 \eta(x, t)}{\partial x^2} + m'' \frac{\partial^2 \eta(x, t)}{\partial t^2} = F(x, t) \quad (2.1)$$

This is a derivation of the equation of motion from Cremer et al. [4] for thin prestressed plates on a Winkler bed using Hamilton's principle:

$$B' \nabla^4 \eta - T' \nabla^2 \eta + s'' \eta + m'' \frac{\partial^2 \eta}{\partial t^2} = p(x, z, t) \quad (2.2)$$

The soft layer of stiffness term, s'' , is neglected. And the pressure term, p , is made into a force by multiplying all terms by the dimension(s) on which the pressure acts.

The solution for free bending waves propagating on the string is used to obtain the wavenumbers, k , of the string. To do this, Eq. (2.1) is solved setting the force term, F , to zero and using an assumption that the displacement will have the form of a wave like such:

$$\partial \eta(x, t) = \eta_A e^{kx} e^{j\omega t} \quad (2.3)$$

The notation used in Eq. (2.3) is for a general wave or near-field. The direction of wave travel or near-field attenuation is determined by the value of k and is shown in Eq. (2.4). Using this notation simply makes derivations of Eq. (2.3) easier.

There are four unique solutions to Eq. (2.1) when using the assumption in Eq. (2.3). These are:

$$k = \begin{cases} \mp j \sqrt{\frac{-T}{2B} + \sqrt{\frac{T^2}{4B^2} + \frac{\omega^2 m'}{B}}} \\ \mp \sqrt{\frac{T}{2B} + \sqrt{\frac{T^2}{4B^2} + \frac{\omega^2 m'}{B}}} \end{cases} \quad (2.4)$$

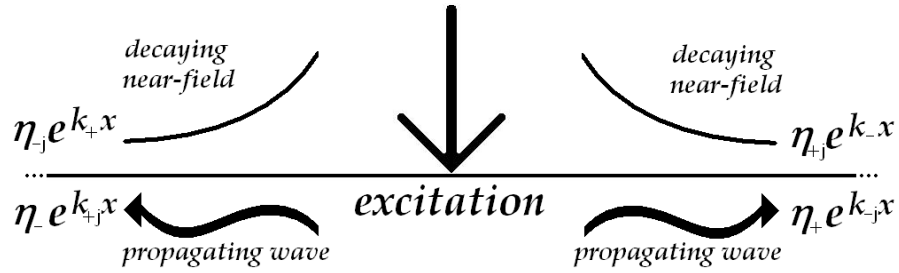


Figure 2.1: Notation for propagating waves and decaying near-fields.

The four different solutions of Eq. (2.4) represent two waves and two near-fields on the string. The first two solutions are the wavenumbers for propagating bending waves in the positive and negative x -directions respectively. The next two solutions are wavenumbers describing the near-fields, which exponentially decay from their respective points of excitation (due to the presence of a boundary condition, e.g. an applied force or a string termination). The notation for the direction and type of wave/near-field can be observed in figure 2.1. The general equation for the total displacement of a beam or string is then a superposition of these four different wave types and can be written as:

$$\eta(x, \omega) = \eta_+ e^{k_- x} + \eta_- e^{k_+ x} + \eta_{j+} e^{k_- x} + \eta_{j-} e^{k_+ x} \quad (2.5)$$

The string is restrained at each end of the string, so supports must be included in the model. A choice was made here to couple the string with two high impedance beams as supports for the string to include energy dissipation through the sound board (including sound radiation). High impedance denotes the beam's impedance is large relative to the impedance of the string. This will allow some of the energy from the string to transmit through the support, while most of the energy is reflected back within the string.

The support-beams are modeled similarly to the string and will contain similar solutions of Eq. (2.5). The support-beams are given a fixed-end boundary condition. This requires a propagating wave and corresponding near-field in the reflected direction from the fixed end of each support-beam to be included. The damping of the beams is then made very high to limit energy coming back into the string from the support-beams.

Eq. (2.5) is solved for free bending waves; therefore, it is only valid for beams (and strings) free from external forces except at boundaries. Because an excitation

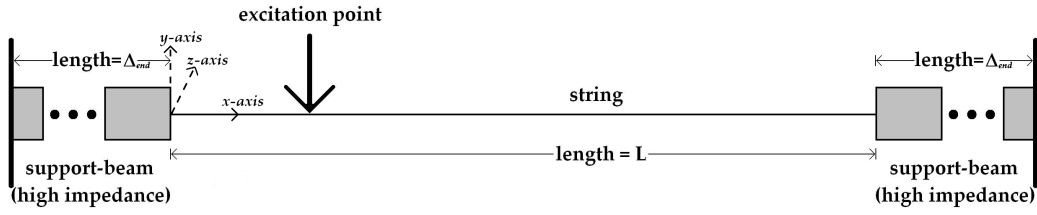


Figure 2.2: Diagram of the string/support-beam model.

is applied at a single point somewhere along the string, the string must be broken up into two separated but coupled segments at the point of excitation. The string/support-beam model is shown in figure 2.2

A problem of numerical instability can result due to the decaying near-field terms and must be addressed. This problem occurs because of the e^{kx} term. When k is real and x is the same sign as k , the value grows exponentially as x becomes larger. If the product of k and x become too large, the term approaches infinity. To fix this problem, wave terms that are at risk of this problem are multiplied by:

$$\frac{e^{-k\epsilon}}{e^{-k\epsilon}} \quad (2.6)$$

Here, ϵ is an x -value equal to or larger than any x -value computed for the section in the positive domain and less than or equal to any x -value computed for the section in the negative domain. This will force the term e^{kx} to be less than 1 for all possible x -values of each section. The displacement of the new wave term will then look like the following:

$$\partial\eta(x, t) = \eta' e^{k(x-\epsilon)}, \quad (2.7)$$

where η' is a scaled displacement amplitude equal to:

$$\eta' = \frac{\eta}{e^{-k\epsilon}} \quad (2.8)$$

This adjustment must be made for near-field terms decaying to the left in the positive x -domain and the near-field terms decaying to right in the negative x -domain. Propagating wave terms must also be adjusted for beams with high damping and large wavenumbers as well. However, this does not apply to the present model because although the support-beams contain high damping, the wavenumbers are small.

Applying Eq. (2.6) to Eq. (2.5) in the method discussed above safely enables the representation of beam and string displacement as a function of 1-D space and frequency for each separate section like so:

$$\eta(x, \omega) = \eta_+ e^{k_- j x} + \eta_- e^{k_+ j x} + \eta'_{j+} e^{k_- (x - (-\Delta_{end}))} + \eta_{j-} e^{k_+ x} \quad (2.9)$$

$$\eta(x, \omega) = \eta_+ e^{k_- j x} + \eta_- e^{k_+ j x} + \eta_{j+} e^{k_- x} + \eta'_{j-} e^{k_+ (x - x_{excite})} \quad (2.10)$$

$$\eta(x, \omega) = \eta_+ e^{k_- j x} + \eta_- e^{k_+ j x} + \eta_{j+} e^{k_- x} + \eta'_{j-} e^{k_+ (x - L)} \quad (2.11)$$

$$\eta(x, \omega) = \eta_+ e^{k_- j x} + \eta_- e^{k_+ j x} + \eta_{j+} e^{k_- x} + \eta'_{j-} e^{k_+ (x - (L + \Delta_{end}))} \quad (2.12)$$

Eq. (2.9) is for the left support-beam ($x \leq 0$).

Eq. (2.10) is for the left side of the string ($0 \leq x \leq x_{excite}$).

Eq. (2.11) is for the right side of the string ($x_{excite} \leq x \leq L$).

Eq. (2.12) is for the right support-beam ($x \geq L$).

(Refer to figure 2.2 and B.6 for the identification of the different sections and the origin of x)

2.3 Boundary Conditions

As is seen from Eqs. (2.9)-(2.12), the total string and support-beam system contains a total of four sections (two string sections and two support-beam sections). Each section contains two waves and two near-fields. The amplitudes of the waves/near-fields are unknown and must be solved using the boundary conditions of the sections. The total system contains eight waves and eight corresponding near-fields with unknown amplitudes. Therefore the solution for sixteen unique boundary condition relationships must be found. Using the premise that each neighboring section is coupled and the support-beams are fixed at their respective non-string end, the boundary conditions (BC) become:

Fixed Support-Beams (two locations - 4 BC)

- Displacement is zero at fixed end
- Bending angle is zero at fixed end

String and Support-Beam Coupling (two locations - 8 BC)

- Displacement is the same for neighboring sections at coupled point
- Bending angle is equal for neighboring sections at coupled point
- Moments are equal for neighboring sections at coupled point
- Sum of the forces at the coupled point is zero

String Coupling at Point of Excitation (one location - 4 BC)

- Displacement is the same for neighboring sections at coupled point
- Bending angle is equal for neighboring sections at coupled point
- Moments are equal for neighboring sections at coupled point
- Sum of the forces at the excitation point is equal to zero

For the above boundary conditions, the displacement is defined by Eq. (2.5). The bending angle is defined by:

$$\beta(x, \omega) = \frac{\partial \eta(x, \omega)}{\partial x} \quad (2.13)$$

The Moment is defined by [13]:

$$M_z(x, \omega) = -B \frac{\partial^2 \eta(x, \omega)}{\partial x^2} + T \eta(x, \omega) \quad (2.14)$$

The Force is defined by [13]:

$$F_y(x, \omega) = B \frac{\partial \eta^3(x, \omega)}{\partial x^3} + T \frac{\partial \eta(x, \omega)}{\partial x} \quad (2.15)$$

Applying the relationships in Eqs. (2.13) - (2.15) to the displacement, Eqs. (2.9) - (2.12), help to formulate the boundary conditions. The formulation of the boundary conditions leads to a $[16 \times 16] \cdot [16 \times 1] = [16 \times 1]$ equation system for the string/support-beam model. In the equation system, each row represents one individual boundary condition, and each column represents one wave/near-field type for its corresponding section of the string/support-beam model.

Each element in the right-hand side of the equation system will be zero for all rows except for the row corresponding to the excitation point, x_{excite} . This element will be a frequency dependent input force, $F_{ex}(x, \omega)$. This force term can be any desired value as a function of frequency and location. However, using a unit impulse force as the force input will make it easy to gather useful information from the models compliance:

$$H = \frac{\eta}{F} \quad (2.16)$$

A unit impulse force will also facilitate future changes to the system if a different force at the same excitation point is desired. This can be done using a convolution in the time domain or a multiplication in the frequency domain. More on the adaptation of input forces is discussed in Chapter 3. It should also be noted here that the system is infinitely linear, and it is possible for the displacement output to be unnaturally large. Therefore, the force will need to be scaled to a reasonable displacement output before applying the model to a desired situation. This will also be explained in Chapter 3.

2.4 Results

The output of the transverse wave model is very dependent on the values assigned to the string and support-beam properties as well as the excitation force. All properties of the string and support-beams can be freely changed (within computational limits), and some small changes (most notably damping terms) to certain properties can drastically change the model output. The string properties include tension, T , mass per unit length, μ , Young's modulus, E , string length, L , and string thickness, d . The properties of the support-beams are the same as the string, except the support beams do not include tension. The model string properties and parameters are

based on those of the actual string used in the measurements, though, some were adjusted slightly to match the resonant frequency of the measured data. Properties of the support-beams represent the entire structure of the instrument and can not be based on factual data. Therefore these properties of the model are purely determined to meet the needs of the model.

For the model to accurately represent the physics of an actual string, properties of the model should agree to strings containing similar properties. Bending stiffness, B , is a property that causes wave dispersion as the value increases. It is computed by the product of the Young's modulus, E , and the cross-section, S . One effect of dispersion is the distance between successive overtones increases with frequency as the bending stiffness increases. This effect is caused by the wave speed of bending waves increasing with frequency and becomes greater as the bending stiffness becomes larger in value [4].

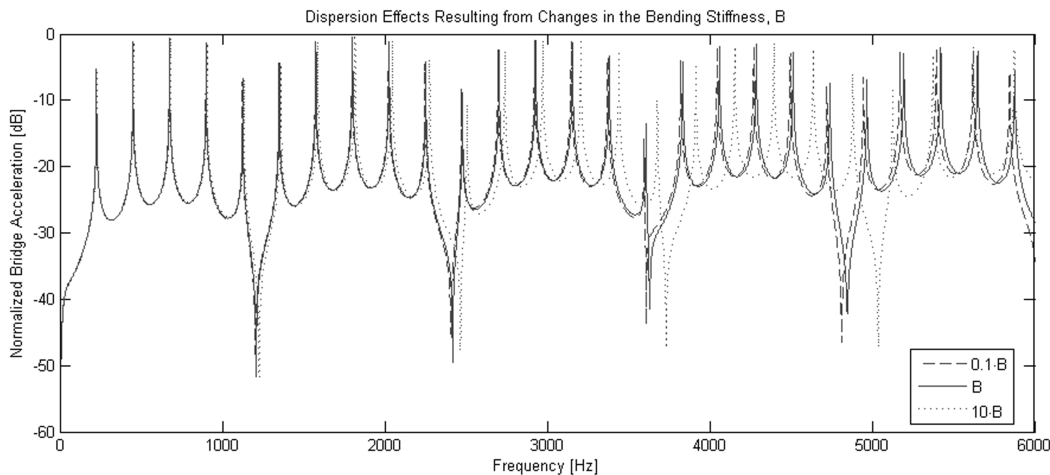


Figure 2.3: Effects of Dispersion for Different Bending Stiffnesses.

It can clearly be seen in figure 2.3 that the present model shows effects of dispersion as the bending stiffness increases. This is a good indication that the model is similar to a natural string with regard to bending stiffness.

Energy losses of the string model are only a result of energy that is transferred to the support-beams and energy that is removed due to damping, i.e. imaginary terms given to the string and beam properties. Similarly, energy losses in an actual string are caused by:

- damping and friction within the string, resulting in heat generation,

- losses to the string supports through transmission, which ultimately results in losses to the instrument structure (including sound radiation),
- and losses due to viscosity in the surrounding air (also a form of heat generation and sound radiation).

An accurate way of modelling these energy losses does not exist without adding more degrees of freedom to the model. Therefore, in the present model, after the real part of the string and support-beam properties and parameters were determined, the damping terms (imaginary part) of string tension, bending stiffness, and mass per unit length were adjusted and re-adjusted many times to best match the acceleration output of the model to the acceleration measured from the single string instrument apparatus (see Appendix A). This comparison was based visually by comparing the respective spectrograms of the measured and modeled accelerations and also audibly by comparing the sound output from each of the accelerations. Spectrograms comparing the measured and modeled accelerations with an impulse excitation (see Chapter 3 for more on modeled excitation forces) can be seen in figure 2.4.

Figure 2.4 shows that there exist similarities as well as obvious differences between the measured and modeled responses. Both signals were normalized in order to gain a better comparison.

Similarities between the simulated and measured spectrograms are:

- The eigenmodes are similar if not the same. Very little effects from dispersion can be seen.
- Higher frequencies decay faster in time than lower frequencies. The decay trends are very similar for both the measured and simulated responses.
- The fundamental frequency is present throughout the entire response time and is dominant (compared to the other frequencies) in the later part of the response but not necessarily in the beginning of the response for both the measured and modeled responses.

Differences between the simulated and measured response spectrograms are:

- More character and uniqueness exist between the individual eigenmodes of the measured response compared to the simulated response. This is most

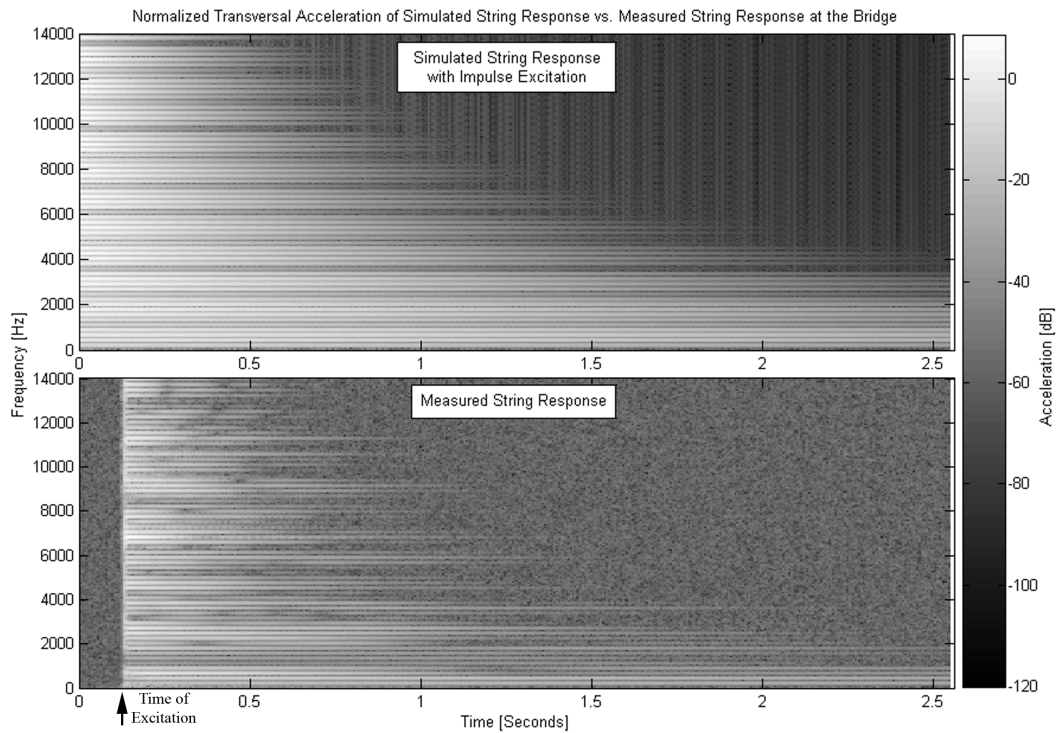


Figure 2.4: Spectrograms comparing the model's impulse response and the measured acceleration.

likely a contribution from the response of the wood structure. The wood structure is not completely rigid and will have resonances of its own, contributing to the signal measured by the accelerometer. The accelerometer is also attached to the wood on the bridge and not directly on the string. This transfer path from string through wood will also change the measured spectrum.

- The anti-resonances for the measured and simulated responses do not occur at the same frequencies. The anti-resonances are dependent on the location where string is plucked relative to the length of the string [12]. This suggests the simulated excitation was plucked at a different relative location than that of the measured excitation. It was intended to excite both the physical and simulated model at one-fifth the length of the string, but it appears the excitation was off slightly on the physical model.
- The simulated model shows a response that has more prominent resonances, i.e. the eigenmodes contain more energy relative to other frequencies. This is because the measured system is not an ideal system, which causes energy

to spread to more frequencies other than resonances and also because the simulated response does not contain any noise.

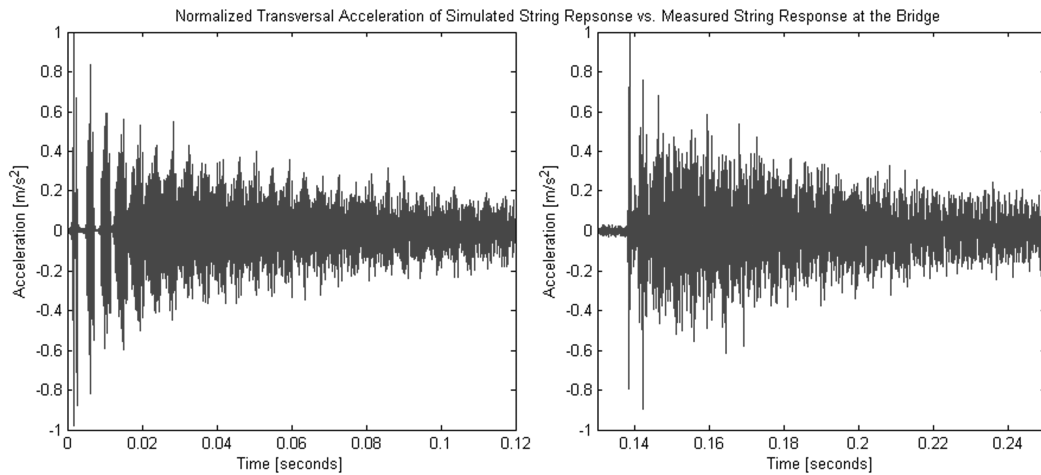


Figure 2.5: Time responses of the modeled and measured accelerations.

Some of these similarities and differences can also be heard when listening to the sound samples generated from these acceleration signals. Most notably, the measured signal has a sound with more body, and one can almost hear the effects of the wood structure, whereas the simulated response signal can be perceived as only a string.

Surprisingly, some similarities can also be seen in figure 2.5 between the accelerations of the measured response and the modeled impulse response in the first 0.1 seconds of the time domain.

As will be discussed in Chapter 3, the type of excitation used makes a considerable difference in the string's response. The model's acceleration when excited with a 10 ms, linear excitation force, as seen in figure 2.6, is noticeably different than the model when excited with an impulse force. The most prominent difference in figure 2.6 is seen in the fundamental frequency and the first few overtones, which are more dominant than the higher overtones ($\sim 6 - 10$ dB). The fundamental frequency and all overtones with an impulse excitation (figure 2.4) are more balanced and equal in magnitude. This difference between responses to the different excitations seems reasonable. An impulse force with an infinitesimally small excitation time will excite all frequencies with the same magnitude, and as the excitation time becomes longer, the excitation energy in the low frequencies will be larger than that of higher frequencies.

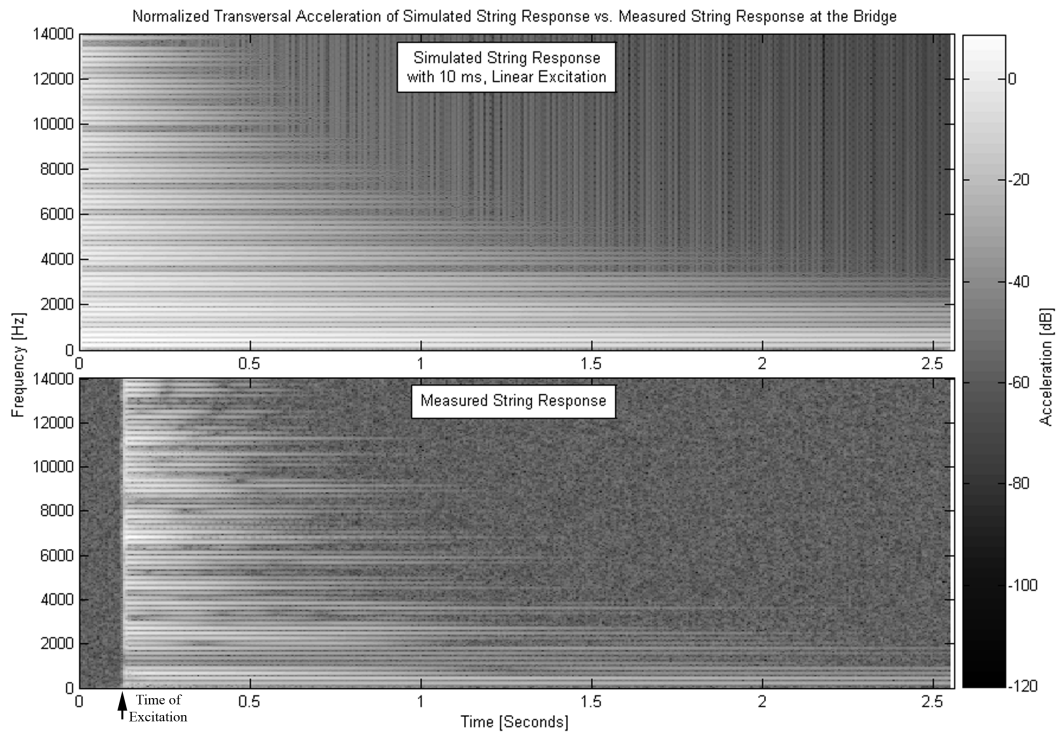


Figure 2.6: Spectrograms comparing the model's response in response to a 10 ms, linear excitation and the measured acceleration.

The model with a 10 ms, linear excitation does appear to be better at modeling the damping trends of the individual frequencies, but this can't be heard in the audio file because the fundamental and first few overtones are too dominating. These differences help support the importance of the type of modeled excitation used.

Chapter 3

Adaptation of Input Force

The transverse vibration model developed here is very malleable. One benefit is almost any desired input force can be implemented into the system. However, determining what input forces are best and most accurately represent a genuine excitation is a very challenging problem. The desired input force for this model is one that represents the resulting forces from a plucked string using a jack and plectrum like the measurement apparatus shown in figure 3.1 and discussed in Appendix A.

One idea to determine the force that is input into the string is to find the dynamic motion of the string during the “pluck”, and then determine the force needed to obtain that same motion from the model. However, there are many problems when attempting to do this. Some problems are capable of being avoided and others are not.

The size and motion of the string prevents measuring the string’s displacement with a displacement laser. The plectrum itself bends during the excitation, which prevents measuring it with the displacement laser as well (see figure 3.2). Therefore, the most accurate degree of displacement that can be measured is that of the jack. This, however, does not give much accuracy for the strings displacement because the jack, plectrum, and string do not move as one rigid system.

One difficulty that can be overcome is measuring the time that the plectrum and string are in contact during excitation. This is accomplished by creating a circuit with the plectrum and string, as can be seen in the figures. 3.3 and 3.4. The voltage supply to the circuit is a 9 Volt battery, and the wire used is a bare copper wire. The wire on the plectrum is fed through the back of the jack and is adhered to the

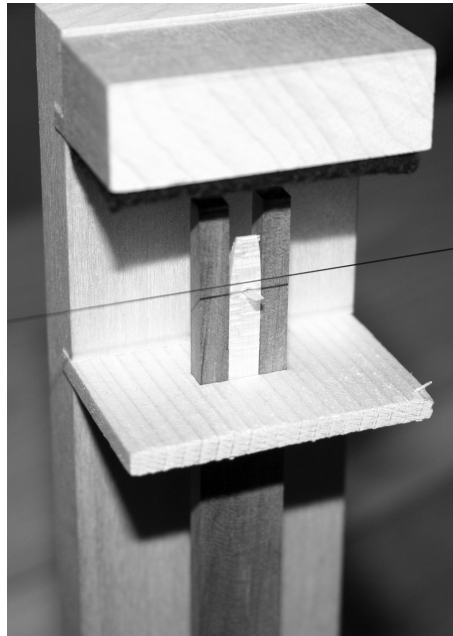


Figure 3.1: Image of the jack, plectrum, and string.

plectrum using a conductive paint.

The circuit remains open when the plectrum and string are not in contact and is only closed when the two are in contact. This produces a DC voltage signal that is measured simultaneously with the accelerometer signal on the bridge (vertical orientation to measure the transversal waves) and the displacement laser signal of the jack. This, in principle, allows the amount of time the plectrum and string are in contact during excitation to be accurately measured. It also allows one to view the

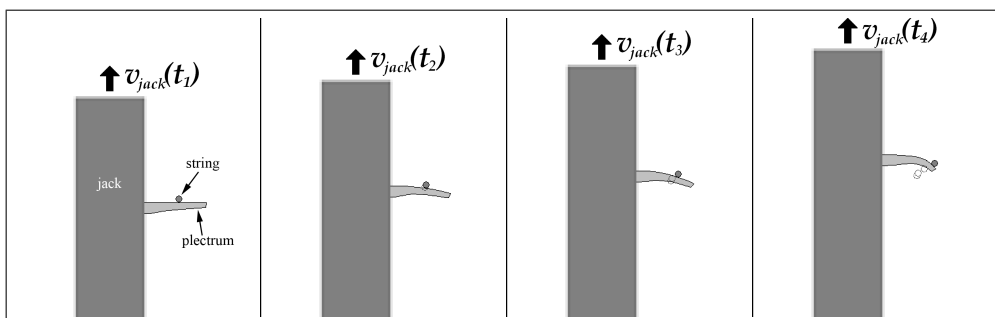


Figure 3.2: Hypothetic cross-sectional view showing the dynamics of the jack, plectrum and string during excitation.

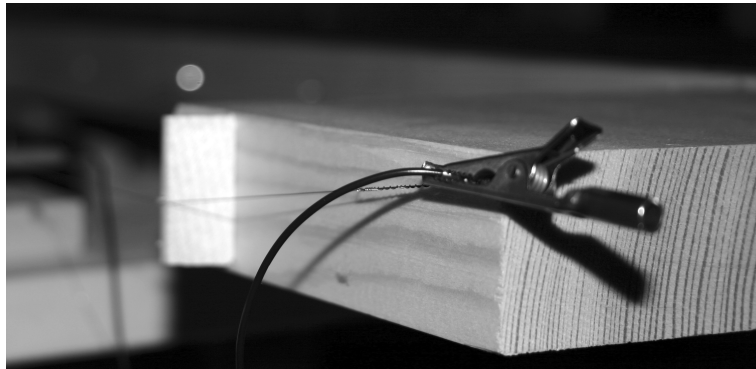


Figure 3.3: Image of wire attached to the string.

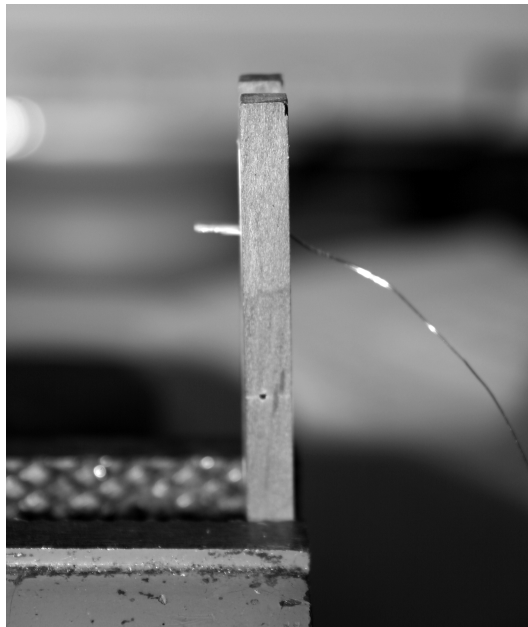


Figure 3.4: Image of wire attached to the plectrum.

response of the string relative to the different stages of plectrum and string contact.

Even though the measured displacement of the jack using a displacement laser cannot be used in the model, it is interesting to observe and gain an understanding of the dynamic motion of the jack. The displacement of the jack (figure 3.5), at first glance, appears to travel almost linearly through the excitation. However, looking at the velocity of the jack (figure 3.6) computed with a difference approximation, one can see that there is in fact a significant change in velocity during the excitation.

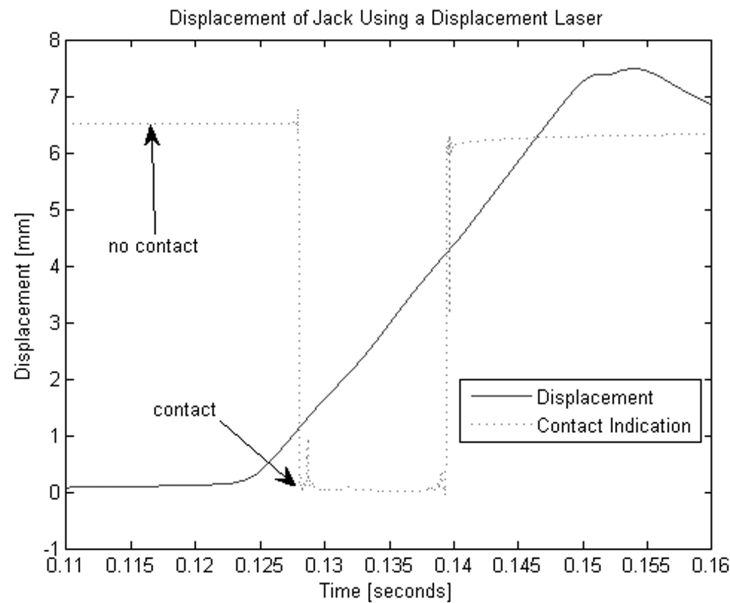


Figure 3.5: Displacement of the jack during string excitation obtained using a displacement laser.

One idea to accurately obtain the string and plectrum displacement is to use a high frame-rate camera. This equipment was unfortunately unavailable, so these tests were not performed. If one could obtain the actual motion of the string during the plectrum and string interaction, the next difficulty is to gain a model of the force that is required to give the observed displacement in the string model. This can be done in the time domain using the known impulse response of the model and using a control method applied to the model analyzing the force required at each time step to get the correct displacement of the string. The computed force would then be convoluted with the compliance of the impulse response model to get the entire response of the model due to this excitation force.

Another difficulty when modeling the excitation force is including the initial contact between the plectrum and the string as well as modeling the moment when the plectrum releases from the string. This later difficulty is of high importance because of the amount of energy that is contributed to the excitation frequencies. Effects of different input forces to the model and the resulting acceleration at the bridge are discussed in Section 2.4.

In figure 3.7, one can see the response of the string at the bridge due to the initial contact from the plectrum and the response of the string at the bridge after the

plectrum releases from the string. It should be noted that the accelerometer on the bridge is oriented in a vertical direction to measure the string's transverse wave motion.

The moment the plectrum releases from the string ($t \approx 0.138s$ seconds) actually shows some very interesting characteristics. The contact signal shows a loss of voltage and then gains voltage again about 1 ms later. This would suggest the string releases from the plectrum and comes back into contact again 1 ms after the initial release.

The peculiarities about this contact observation are:

- This phenomena was observed in all the contact measurements including changes of the battery, the tension of the string, and the sampling frequency.
- It is not very likely for the string to come and hit the plectrum again after the plectrum release because the jack and plectrum are allowed to move completely past the string and out of the way of the string.
- There is a slight increase in magnitude of the measured acceleration after the first "release point" and then another increase in magnitude after the sec-

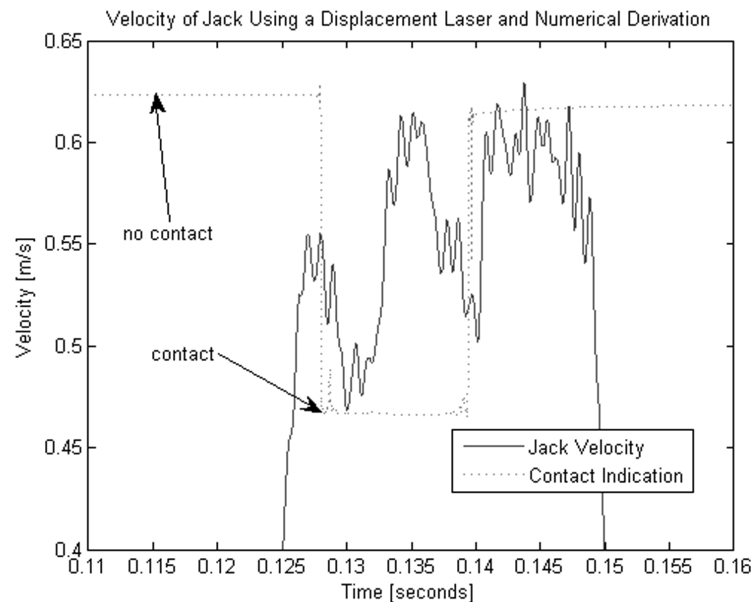


Figure 3.6: Velocity of the jack during string excitation obtained using a displacement laser.

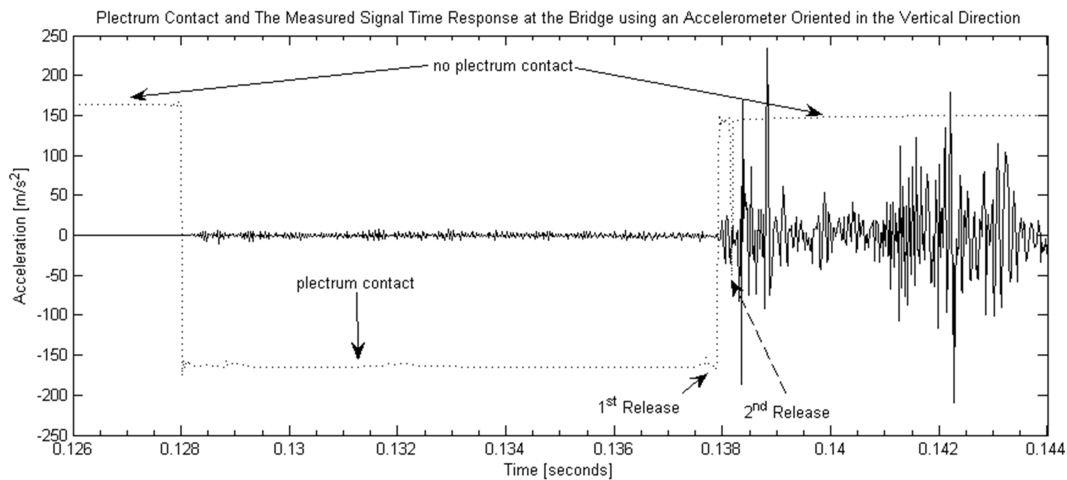


Figure 3.7: Transverse wave response measured at the bridge and a plot indicating the contact of string and plectrum.

ond “release point”. This suggests that there are two separate interactions between the string and plectrum during the release. The transversal wave speed is about 320m/s , and the length of the string is approximately 0.695m . Since the string was excited at about one-fifth its length, the shortest period for a transversal wave to travel from the excitation point to the bridge and back is approximately $0.8 - 0.9\text{ms}$. The length of total contact time is around $1.0 - 1.1\text{ms}$. This suggests that it is possible for a reflected transversal wave to cause the string and plectrum to lose contact with one another before the plectrum moves completely past the string.

- The figure shows a delay before responding to the initial plectrum contact at $t \approx 0.128\text{s}$. This would suggest that there should also be the same length of delay after the string releases from the plectrum because the transversal waves on the string should move with the same velocity regardless of magnitude. There is no delay after the first “release”, but there appears a delay after the second “release point” suggesting that the true complete release occurs after the second.

Even though a partial analysis of the measurements can be made, there is still the question of whether this is a physical or electrical phenomenon or if it is just a poor testing method. If it is indeed physical, one must wonder how much of an effect this has on the resulting string response and whether or not it can or should be modeled.

Since the motion of the string could not be measured, a simple excitation input force was used with assumptions that the string tension and the string velocity at the excitation point are constant. It is known that the velocity of the string at the excitation point is not constant, but it was decided that a simple velocity approximation was better than forcing a complex input force on the model. The equation with these simple assumptions forms Eq. (3.1), a linearly increasing excitation force for small displacements.

$$F_{ex} = T_0 \left[\sin \left(\tan \left(\frac{v_{string} \cdot t}{x_{ex}} \right) \right) + \sin \left(\tan \left(\frac{v_{string} \cdot t}{L - x_{ex}} \right) \right) \right] \quad (3.1)$$

The different input forces used for the model excitation are shown in figure 3.8. This figure shows the linear force of Eq. (3.1), as well as an impulse force at $t = 0$ and a parabolically increasing force proportional to time for the duration of the contact time, $F_{ex} = t^2$.

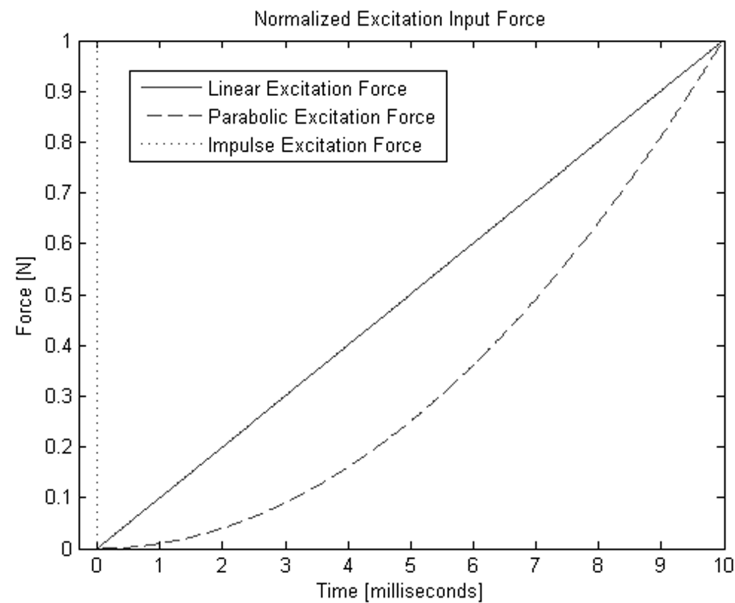


Figure 3.8: Different input forces used to excite the string model.

As was mentioned at the end of Section 2.2, the input force needs to be scaled to prevent a response that is out of proportion with actuality. This is done by finding the displacement of the string, $\eta(t, x)$, at the end of the modeled excitation time, in response to any chosen input force. This chosen input force is then multiplied by

the ratio of a reasonable displacement ($\sim 1 - 1.5\text{mm}$) and the current displacement (Eq. (3.2)). The string's displacement due to a chosen input force is calculated using a simple inverse fast Fourier transform for a defined excitation point, x_{ex} , and then convoluting that impulse response with the current chosen input force.

$$F_{excitation,new} = F_{excitation,old} \left(\frac{\eta_{desired}}{\eta(t_{contact,end}, x_{excitation})} \right) \quad (3.2)$$

To apply this new scaled input force to the model, it is kept in the time domain and is convoluted with the impulse response of the model's dynamic compliance (Eq. (2.16)) at a chosen value of x as show in Eq. (3.3).

$$\eta(x, t) = \left[\frac{1}{2\pi} \int_{-\infty}^{\infty} \eta(x, \omega) e^{-j\omega t} d\omega \right] * F_{excitation,new} \quad (3.3)$$

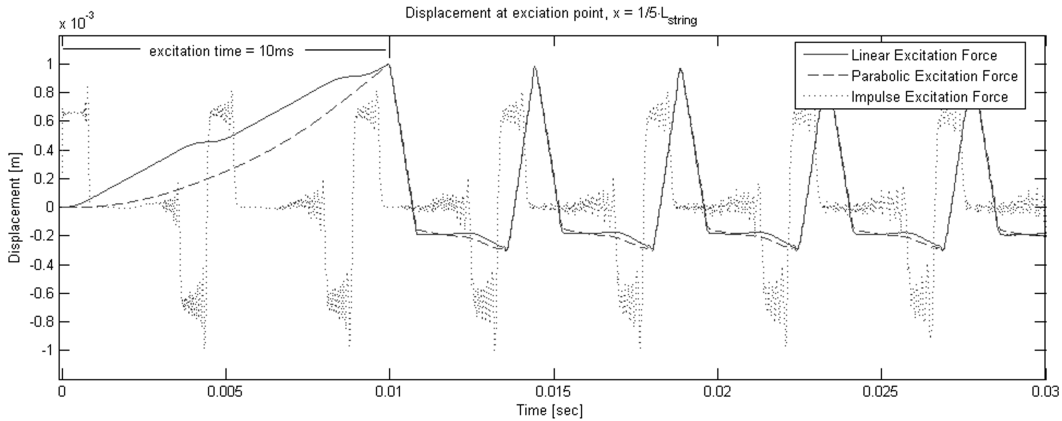


Figure 3.9: String response at excitation point due to the different excitation forces used in the model.

Figure 3.9 shows the scaled time responses of the string at the excitation point due to the different input forces of figure 3.8. The excitation time is the same for all input forces (10ms), except for the impulse force which only occurs at time $t = 0$. It is interesting to see that the linear excitation force and the parabolic excitation force behave quite differently during the excitation time (initial 10ms). The string, in response to a parabolic excitation force, behaves like a mass with no resonance characteristics, whereas the string's response to a linear excitation force appears to be very affected by the resonance of the string at the strings resonance frequency. This is noticed by the small deviations the string response takes from a linear growth.

Chapter 4

Longitudinal Wave Model

4.1 Formulation

The longitudinal wave model, as mentioned before, is largely based on work performed by Baláz Bank and László Sujbert. The longitudinal waves are a result of the periodic elongation of the string due to the motion of the transversal waves. The longitudinal waves excited will contain forced response frequency components, which are dependant on the transverse wave frequencies and free response frequency components at the longitudinal wave string eigenmodes. Transverse to longitudinal wave coupling is simplified by limiting the transfer of energy in only the direction of transverse vibrations to longitudinal vibrations. This assumption is valid as long as the longitudinal vibration is small compared to the transverse one.

An approximation of the longitudinal vibration can be characterized by Eq. (4.1) as derived in [2].

$$\mu \frac{\partial^2 \eta(x, t)}{\partial x^2} = ES \frac{\partial^2 \eta(x, t)}{\partial x^2} + \frac{1}{2} ES \frac{\partial (\partial \eta / \partial x)^2}{\partial x} \quad (4.1)$$

This standard, one-dimensional wave equation with an additional force term shows that the transverse string motion can only excite longitudinal vibrations if the transverse displacement is large.

According to Eq. (4.1), the transverse to longitudinal excitation force distribution,

$F_{t \rightarrow l}(x, t)$, is computed as:

$$F_{t \rightarrow l}(x, t) = \frac{1}{2}ES \frac{\partial [\partial \eta(x, t) / \partial x]^2}{\partial x} \quad (4.2)$$

For this model, the force coupling equation is best performed in the time domain by examining the string shape at each successive time-step. To approximate Eq. (4.2), differentials were replaced by finite difference schemes.

After the resolution of the finite difference computation is determined, the time response for each point x can be computed according to Eq. (3.3) using an inverse fast Fourier transform (ifft) in place of the inverse Fourier transform.

To perform the finite difference approximations, a second-order-accurate, central difference expression (Eq. (4.3)) is used for the x -values located away from the support-beam boundaries as derived by [14]:

$$\left(\frac{\partial \eta(x, t)}{\partial x} \right)_i = \frac{\eta_{i+1} - \eta_{i-1}}{2(\Delta x)} + O(\Delta x)^2 \quad (4.3)$$

Here, $O(\Delta x)$ is a formal mathematical notation which represents “terms of-order-of Δx ”. It states the accuracy of the difference approximation, i.e. which terms are suppressed.

For the x -value of the string at the left side support-beam boundary, the following second-order-accurate difference expression (Eq. (4.4)) is used [14]:

$$\left(\frac{\partial \eta(x, t)}{\partial x} \right)_1 = \frac{-3\eta_1 + 4\eta_2 - \eta_3}{2(\Delta x)} + O(\Delta x)^2 \quad (4.4)$$

Eq. (4.4) is identical to a second-order-accurate, forward difference expression. Similarly, the x -value of the string at the right side support-beam boundary is a second-order-accurate, backward difference expression (Eq. (4.5)) and is represented as such [14]:

$$\left(\frac{\partial \eta(x, t)}{\partial x} \right)_N = \frac{3\eta_N - 4\eta_{N-1} + \eta_{N-2}}{2(\Delta x)} + O(\Delta x)^2 \quad (4.5)$$

The longitudinal amplitudes resulting from the force determined in Eq. (4.2) are computed for specific longitudinal modes. These modes are dependent on the string properties E , the Young’s modulus and ρ , the string density. Since the model

is for one-dimension and the string is thin, the speed of sound of the longitudinal waves is given by:

$$c_l = \sqrt{\frac{E}{\rho}} \quad (4.6)$$

The modal frequencies are thus given by:

$$f_{n,l} = \frac{nc_l}{2L} \quad (4.7)$$

The transverse to longitudinal force is then calculated for each mode of the longitudinal waves, k . This is determined by the expression:

$$F_{t \rightarrow l,k}(t) = \int_0^L F_{t \rightarrow l}(x,t) \sin\left(\frac{k\pi x}{L}\right) dx \quad (4.8)$$

The instantaneous amplitude of the longitudinal wave mode, ζ_k , is given by:

$$\zeta_k(t) = F_{t \rightarrow l,k}(t) * \zeta_{\delta,k}(t) \quad (4.9)$$

Where $F_{t \rightarrow l,k}(t)$ is a coupled modal force from Eq. 26, and $\zeta_{\delta,k}(t)$ is the impulse response of a longitudinal wave defined by:

$$\zeta_{\delta,k}(t) = \frac{1}{\pi L \mu} \frac{e^{-t/\tau'_k}}{f'_k} \sin(2\pi f'_k t) \quad (4.10)$$

The total longitudinal displacement is then calculated by the expression:

$$\zeta(x,t) = \sum_{k=1}^{\infty} \zeta_k(t) \sin\left(\frac{k\pi x}{L}\right) \quad (4.11)$$

4.2 Model

Computing the transverse to longitudinal excitation force, Eqs. (4.2) and (4.8), and the instantaneous amplitude of the longitudinal displacement, Eq. (4.9), is a heavy load on both the computer's processor and memory. Convolutions, inverse fast Fourier transforms, and time and space resolution all contribute to the computational load. To reduce this load, the equations are rearranged, and/or combined and the string is evaluated in groups of points on the string rather than individual points on the string (see Appendix B.4 and B.5).

The outputs of the longitudinal wave model are the displacements of the longitudinal waves as a function of space and time. They themselves are not of much interest, but the resulting forces at the bridge due to these displacements are of high importance. These longitudinal forces will be examined in the following chapter, Chapter 5.

Chapter 5

Forces at the Bridge

5.1 Formulation

For stringed instruments, the resulting string forces at the instrument's bridge have a significant influence on the radiated sound. The character of the sound heard from musical instruments is most influenced by the soundboard, which is directly coupled to both the instrument's bridge and the air that propagates the sound to one's ear. If one thinks of the transmission paths between the bridge to ear as a black box containing an infinite number of transfer functions, the main inputs into this black box are the forces at the bridge.

The bridge forces in this model include a vertical force in the y -coordinate domain, due to the transversal vibrations and a horizontal force in the x -coordinate domain, due to the generated longitudinal vibrations.

The longitudinal and transverse forces are computed separately using finite difference approximations in a similar form explained in Section 4.1. The transversal force at the bridge is equal to the shear force within the string and is given by Eq. (2.15) in Section 2.2. The finite difference expressions used for this computation are a second-order-accurate, backward, third difference expression represented in Eq. (5.1) for third derivative approximations [14] and a second-order-accurate, backward, first difference expression given in Eq. (5.2) [9] for first derivative approximations.

$$\left(\frac{\partial^3 \eta}{\partial x^3}\right)_N = \frac{5\eta_N - 18\eta_{N-1} + 24\eta_{N-2} - 14\eta_{N-3} + 3\eta_{N-4}}{2(\Delta x)} + O(\Delta x)^2 \quad (5.1)$$

$$\left(\frac{\partial \eta}{\partial x}\right)_N = \frac{3\eta_N - 4\eta_{N-1} + \eta_{N-2}}{2(\Delta x)} + O(\Delta x)^2 \quad (5.2)$$

The longitudinal force at the bridge is equal to the tension at the bridge and is given by Eq. (5.3)[2].

$$F_l(t) = - \left[T_0 + ES \frac{\partial \xi}{\partial x} \Big|_{x=L} + \frac{1}{2} ES \left(\frac{\partial \eta}{\partial x} \Big|_{x=L} \right)^2 \right] \quad (5.3)$$

One must keep in mind that the magnitudes of the transversal and longitudinal wave forces at the bridge are not directly proportional to sound radiation because the influence of a soundboard is not included in the model. As mentioned before, the influence of radiated sound from transversal and longitudinal string vibrations is dependent on their energy transfer to bending waves in the soundboard.

5.2 Results

The longitudinal string vibration measurements made on the apparatus were unfortunately unusable because of a poor signal to noise ratio. Therefore, comparisons of the model's results to measurements performed on the apparatus were not able to be performed. It was decided that testing the longitudinal model with different inputs would be the next best alternative to view how the model acts. However, it should be noted that making observations of the model's output alone does not suggest anything about the accuracy of the model.

A simple observation that can be made from the longitudinal wave model's output is a spectrogram of the modeled longitudinal wave force on the bridge due to an impulse excitation (using the output from the transverse wave model as the input of the longitudinal wave model). A spectrogram showing this can be seen in figure 5.1.

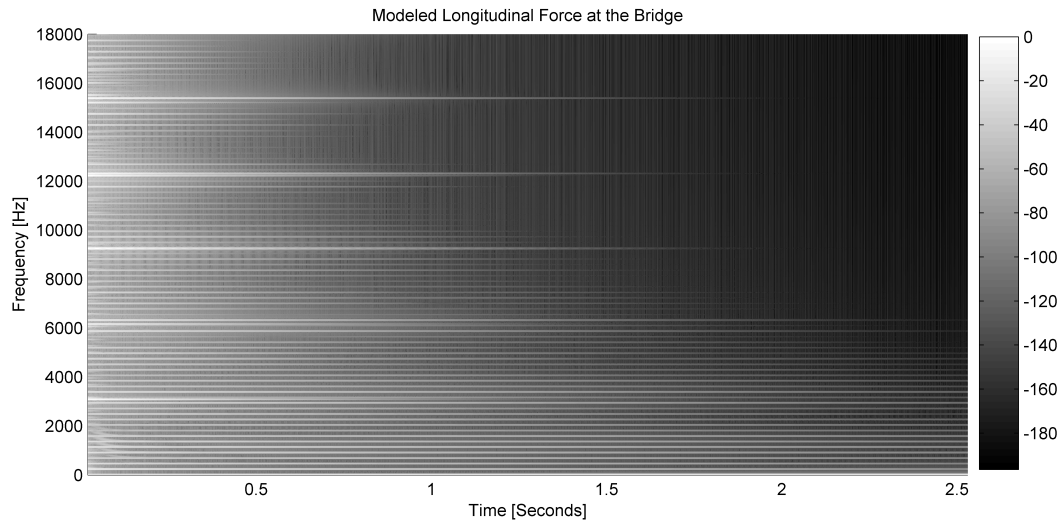


Figure 5.1: Modeled longitudinal wave forces at the bridge as a result of transverse vibrations with an impulse excitation.

Although it is not immediately visible in figure 5.1, there are two different longitudinal forces acting on the bridge. There are the force components due to the longitudinal wave eigenmodes, and there are the components due to the forcing frequencies of the transverse waves.

The longitudinal eigenmodes are located at 3074Hz , 6148Hz , 9223Hz , etc. They begin at $t = 0$, damp out quickly, and are stronger in amplitude than the forcing frequency components. It should be noted that the damping of these eigenmodes is controlled by the modeled parameters, and it is not known if this is a true representation of the physical apparatus because of a lack of measurement data. The components due to the transverse forcing frequencies are therefore the majority of the longitudinal force frequency components.

To better understand the generation of longitudinal eigenmodes as well as the interaction between forced and natural responses, the model was modified to include only specific forcing frequencies. The first modification removed all but one of the transverse frequency components. Figure 5.2 shows the longitudinal forces at the bridge due only to a 900Hz transverse wave component as the input to the longitudinal wave model (900Hz corresponds to the 4th transverse harmonic).

The result of this modification to the model is quite interesting. The spectrogram shows an expected, single forced frequency component, however, the frequency of this component is at twice the frequency of the transverse wave frequency. Mathe-

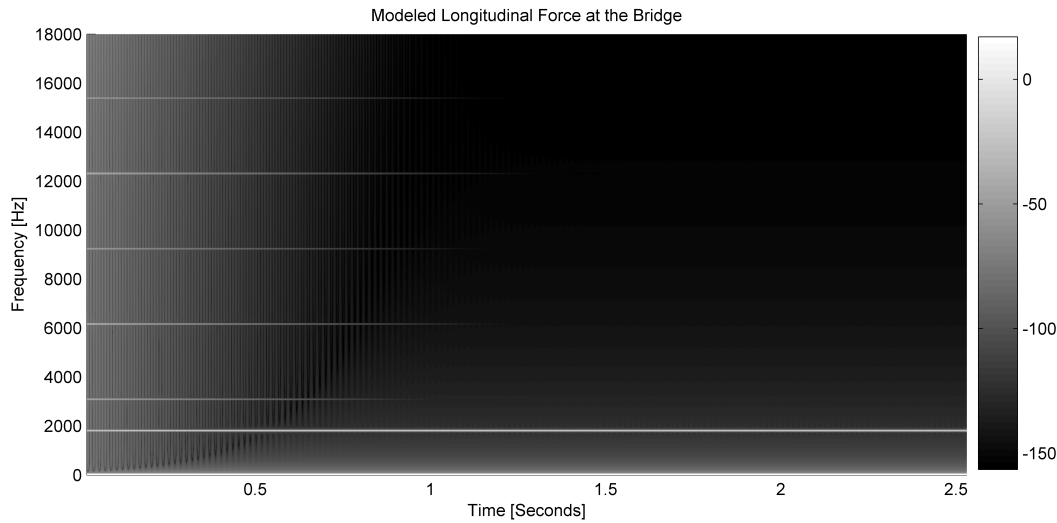


Figure 5.2: Modeled longitudinal wave forces at the bridge as a result of a 900Hz transverse wave component.

matically, the doubling of frequency can be shown through Eq. 4.2. Physically, one can think about the motion of a transverse wave on a string and how its motion generates a longitudinal wave.

In order for a transverse wave to exist, the string must slightly elongate from its resting length. This elongation is the generating force for the longitudinal wave response, and it occurs every half cycle of the transverse vibration. Thereby, every cycle of a transverse wave generates two cycles of a forced longitudinal wave.

Another peculiarity seen in the spectrogram of figure 5.2 is that even though only the 900Hz component of the transverse wave is input into the longitudinal wave model, all longitudinal eigenmodes are excited. It was expected that only the eigenmodes close in frequency would have been excited, however, this is not the case. It is also strange that the forced longitudinal wave response at 1800Hz is present and undamped for the duration of the response, but the longitudinal eigenmodes become damped out.

To investigate these above peculiarities, another modification was made to the model. Again, only a 900Hz transverse wave component was input into the longitudinal wave model, but this time a hanning window was placed on the beginning of the transverse wave excitation frequency component. The result in figure 5.3 shows that with a hanning window at the beginning of the excitation, only the lowest longitudinal eigenmode (3074Hz) is barely present.

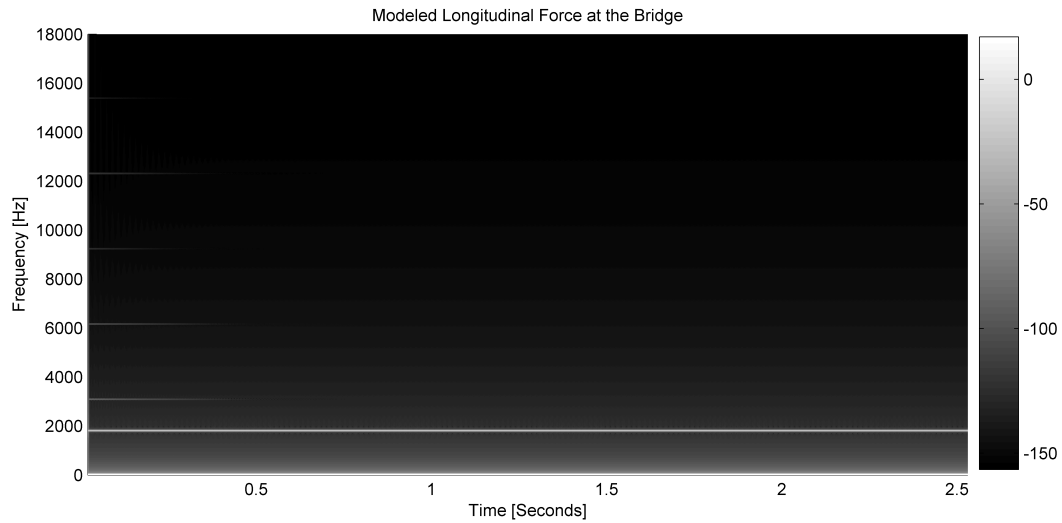


Figure 5.3: Modeled longitudinal wave forces at the bridge as a result of a 900Hz transverse wave component with a hanning window on the beginning of the excitation.

To test the generation of longitudinal eigenmodes further, the model was again run with an impulse excitation (using the output from the transverse wave model as the input of the longitudinal wave model), but this time a hanning window was placed on the beginning of the excitation input.

Figure 5.4 reveals that even with a hanning window on the transverse wave input, longitudinal waves still occur. This again supports the idea that forced frequency components contribute to the generation of the longitudinal eigenmodes and the longitudinal eigenmodes are not formed from only abrupt changes to the system.

Another question that arose was how different transverse wave frequency components interacted with each other in the generation of longitudinal waves. To test this, the model was run again with the same 900Hz transverse wave frequency component input as well as a 225Hz transverse wave frequency component (225Hz corresponds to the 1st transverse harmonic). The result can be observed in figure 5.5

The spectrogram of two transverse wave frequency components as the input is quite interesting. Figure 5.5 shows the expected longitudinal wave components at twice the transverse wave component frequencies and the longitudinal eigenmodes, but there are also two other forced frequency components present at 625Hz and 1125Hz. This is in agreement with Bank and Sujbert [2] who state that the exci-

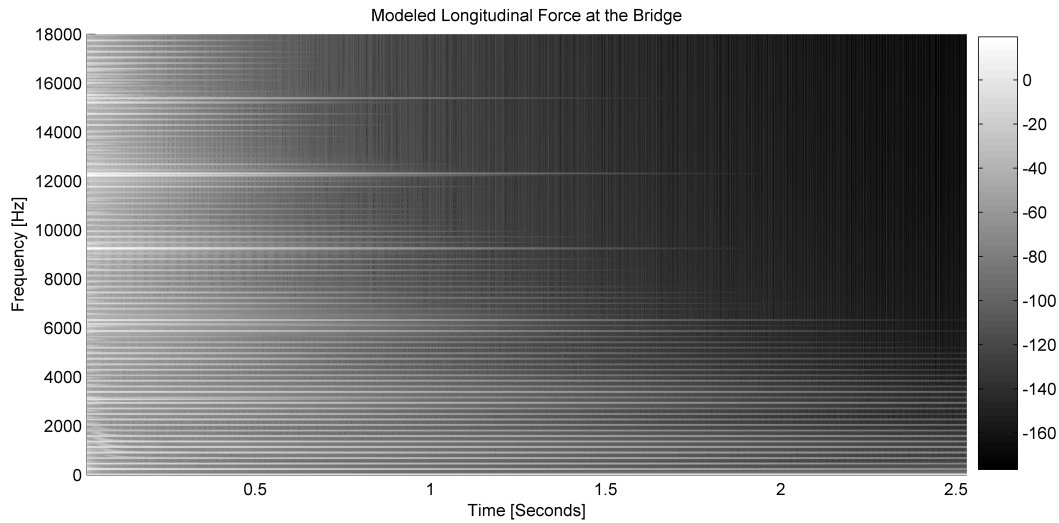


Figure 5.4: Modeled longitudinal wave forces at the bridge as a result of transverse vibrations with a hanning window on the beginning of the excitation.

tation force, $F_{t \rightarrow l, k}(t)$, is non-zero for transverse modes $m + n = k$ and $|m - n| = k$. This is because in all other cases the spatial distribution of the excitation $F_{t \rightarrow l}(x, t)$ is orthogonal to the modal shape of mode k .

To further observe how the forced frequency components excite the longitudinal eigenmodes, the model was again run with a third frequency component at 3155Hz along with the other two components at 225Hz and 900Hz. 3155Hz was chosen because it is located at a frequency near a longitudinal eigenmode. A long hanning window was placed at the start of the excitation to remove effects from abrupt changes to the system. The result shown in figure 5.6 confirms what was expected. Eigenmodes close to forced frequencies were excited (3074Hz and 6148Hz) and other eigenmodes were not. The excitation of these eigenmodes is not as strong as when all transverse frequencies are included in the excitation. This is to be expected though because less energy is present around the eigenmodes since only three frequency components are included in the excitation.

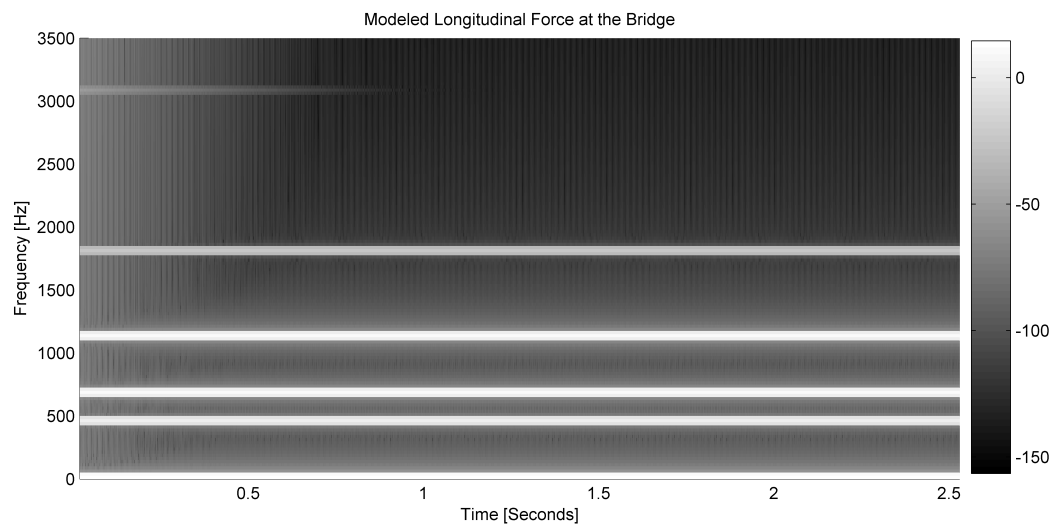


Figure 5.5: Modeled longitudinal wave forces at the bridge as a result of 225Hz and 900Hz transverse wave components as the input.

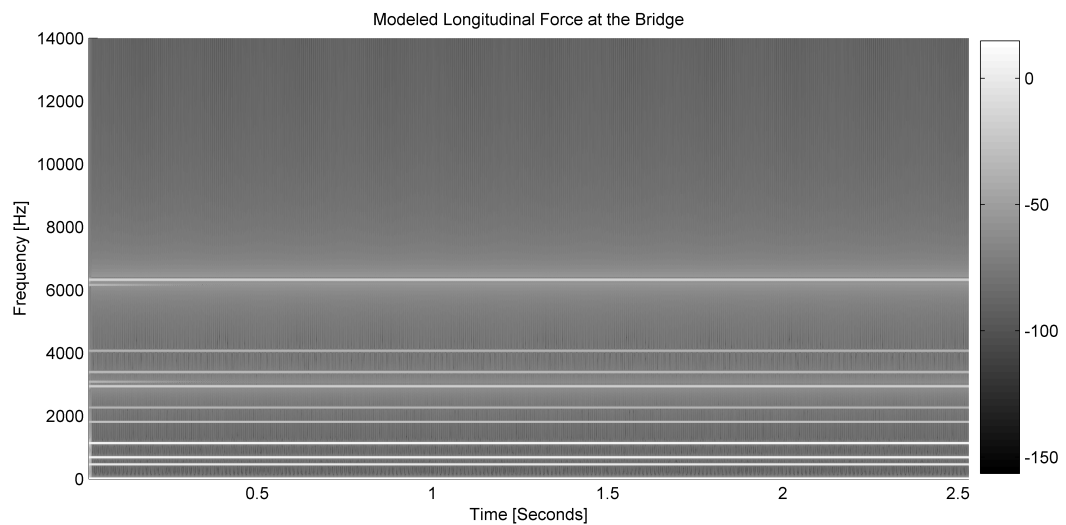


Figure 5.6: Modeled longitudinal wave forces at the bridge as a result of 225Hz, 900Hz and 3155Hz transverse wave components as the input with a hanning window on the beginning of the excitation.

Chapter 6

Conclusions

The developed model appears to work quite well for its purpose of investigating unidirectional coupling of transverse waves and longitudinal waves in stringed musical instruments. It seems to be quite adaptable and malleable to different string properties as well as different excitations. The frequency based transverse wave model appears to be accurate in comparison to the measurements made on the simple one-stringed instrument. Unfortunately, the same statement about the time domain longitudinal wave model cannot be made because of a lack of measurement data.

The longitudinal wave model does prove beneficial in observing how different transverse wave frequencies contribute to the generation of longitudinal waves, though it would definitely be more advantageous if comparisons of the models output to measured results could be made.

The motivation was to investigate the cause and importance of longitudinal forces of a plucked string instruments' bridge. It was inspired by the question that arose during Ben Henley's thesis [7] of whether overlooking horizontal bridge forces contributed to a lack of high frequency sound characteristics when trying to replace a string with shakers.

Although horizontal forces at the bridge do contribute to the sound quality produced by stringed instruments, it is not likely that excluding these forces were the primary explanation to Henley's problem. Although the small mass per unit length (approximately $3.18 \times 10^{-4} \text{kg/m}$) allows for large longitudinal wave amplitudes to develop (Eq. 4.10), the longitudinal modes of a virginal's string are not very dense (approximately every 3000Hz), and the forced longitudinal frequency components

occur at the same frequencies as the transverse frequencies. The sound generated from these longitudinal forces are therefore not likely to be obvious to an untrained listener's ear and are probably not the cause to Henley's problem.

For the sake of understanding the nature of stringed instruments in more depth, it could prove beneficial to perform more research in these subject areas using the methods, measurement apparatus and possibly the model used here.

Certainly, it would be very rewarding to have longitudinal measurement data from the single stringed instrument used in the measurements to compare with the model. Separating the jack and plectrum from the string and body of the instrument was very helpful in discerning the origins of different vibrations. It may also be very advantageous to research the plectrum excitation in depth to understand the interaction between plectrum and string as well as the resulting sound characteristics from different types of excitations.

The developed model may be helpful to instrument builders to observe effects of different plectrums, strings and possibly jack mechanisms. It is very adaptable to different situations, but it is difficult to say without more research if the model is more advantageous than other methods such as a finite difference model.

Bibliography

- [1] Anders Aseknfelt. 5 lectures on the acoustics of the piano, 1990. Available from http://www.speech.kth.se/music/5_lectures/contents.html (Accessed Feb 2007).
- [2] Balázs Bank and László Sujbert. Generation of longitudinal vibrations in piano strings: From physics to sound synthesis. *J. Acoust. Soc. Am.*, 117:2268–2278, 2005.
- [3] A. Chaigne. On the use of finite differences for musical synthesis. application to plucked stringed instruments. *J. Acoustique*, 5:181–211, 1992.
- [4] Heckl M. Cremer, L. and B.A.T. Petersson. *Structure-Borne Sound - Structural Vibrations and Sound Radiation at Audio Frequencies*. Springer-Verlag, 3rd edition, 2005.
- [5] S. Van Duyne and J. O. Smith. Physical modeling with the 2-d digital waveguide mesh. In *In Proc. Int. Computer Music Conf (ICMC'93)*, pages 40–47, 1993.
- [6] N. Giordano and A. J. Korty. Motion of a piano string: Longitudinal vibrations and the role of the bridge. *J. Acoust. Soc. Am.*, 100:3899–3908, 1996.
- [7] B. Henley. Not yet published. Master's thesis, Division of Applied Acoustics, Chalmers Teknisk Högskola.
- [8] L. Hiller and P. Ruiz. Synthesizing musical sounds by solving the wave equation for vibrating objects. *J. Acoust. Soc. Am.*, 19:462–470, 1971.
- [9] Klaus A. Hoffman and Steve T. Chiang. *Computational Fluid Dynamics For Engineers*, volume 1 of 2. Engineering Education System, 1995.
- [10] E. Lindberg. Solving inverse problems in time domain with the lms algorithm - estimation of excitation forces. Master's thesis, Division of Applied Acoustics, Chalmers Teknisk Högskola, 2006.

- [11] Philip M. Morse. *Vibration and Sound*. McGraw-Hill Book Company Inc., 1936.
- [12] Thomas D. Neville H., Rossing. *The Physics of Musical Instruments*. Springer, 2nd edition, 1998.
- [13] Alf Samuelson and Nils-Eric Wiberg. *Finite Element Method Basics*. Studentlitteratur, 1998.
- [14] John F. Wendt and John David Anderson. *Computational Fluid Dynamics: An Introduction*. Springer-Verlag Telos, 2nd edition, 1996.

Appendix A

Measurement Apparatus

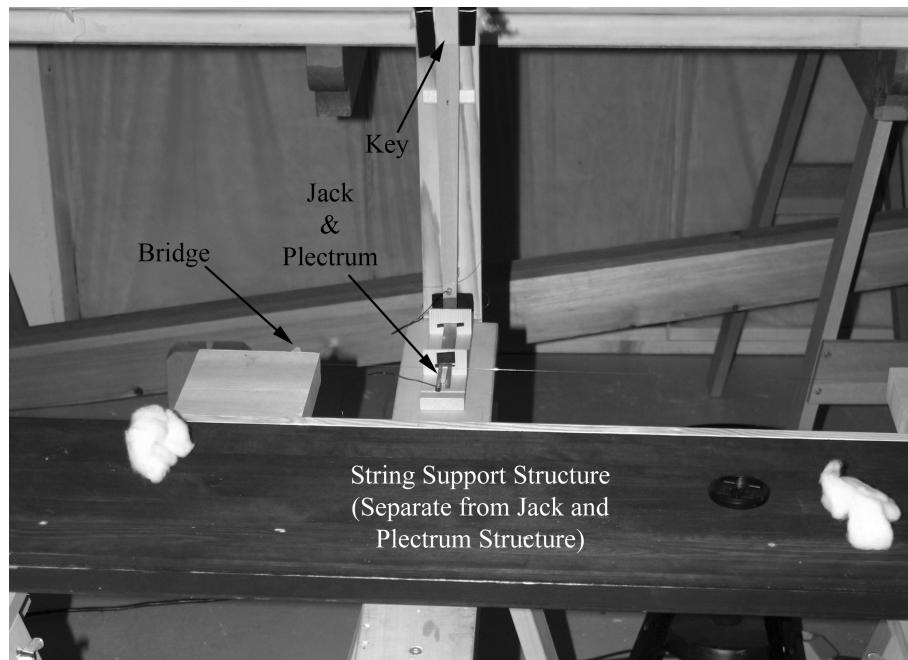


Figure A.1: The measurement apparatus (Front View).

The instrument used in our measurements, built by Gregor Bergmann, is made of wood and contains only one string ($\mu = 3.18 * 10^{-4} kg/m$). The string is tensioned by hanging weights with a known mass on one end. The entire apparatus is modified so the jack and plectrum are completely separated from the stringed part of the instrument. This assures that all measured accelerometer signals at the bridge comes from string vibrations and not vibrations from the jack or key. This is very

important when looking at the early instances of the string's response.

The primary interest of the measurements is to obtain information about transversal and longitudinal vibrations of a single string. Therefore, it is important to isolate these vibrations from vibrations of other parts of the instrument such as soundboard, other strings, structure, keys, etc. Most vibrations other than the string's were isolated. However, the wood structure, which the measurement instrument was mounted upon, contains its own resonances, and some effects of the structure are present in the measured signals. These effects are discussed in Section 2.4.



Figure A.2: The measurement apparatus (Side View).

Appendix B

MATLAB Code

B.1 Wavenumber and Coefficient Calculations

```
% This workspace will numerically calculate the wave numbers and
% coefficients for the plectrum & string interaction. The string is broken
% into two coupled segments. Located at the left side of segment 1 and the
% right side of segment 2, are highly-damped, large impedance beams
% connected at their respective ends to prevent any total non-zero
% displacement

home
clear all
warning('off') % To prevent the display of the eps warning
ssize = get(0,'screensize');
%%%%%%%%%%%%%%%%%%%%%%%%%%%%%%%%%%%%%%%%%%%%%%%%%%%%%%%%%%%%%%%%%%%%%%%%

B_change = 1;
T_change = 1;
f_change = 1;
% String Properties
T23 = 4.3*9.8*(1*T_change+j*0.00002); % Tension (mass*gravity)
T14 = 0;
T_mu = real(T23);
L = 0.695; % String Length
f_string = 224.61*f_change; % Resonant frequency of string
m_per_l = real(T_mu)/(f_string*2*L)^2; % actual string ~ 3.18e-4 kg/m

% Segment 2 and 3 (String)
```

```

E23 = 190e9; % Young's Modulus
diam23 = 0.00023; % String Diameter
mu23 = m_per_l*(1-j*.0003); %*pi*(diam23/2)^2/L; % Mass/unit length
inert23 = 1/4*pi*(diam23/2)^4; % Inertia for a small cylindrical plate
BB23 = inert23*E23*(1*B_change+j*0.00035); % Bending Stiffness
rho23 = m_per_l/pi/(diam23/2)^2;

save string_prop.mat E23 BB23 T23 rho23

damp_end = (1+j*1000);
del_end = 10*L;
% Segment 1 (Left Side MASS)
E1 = 250e10; % Young's Modulus
mu1 = 0.05-0.03*j; % Mass/unit length
diam1 = .007; % Side Diameter
inert1 = 1/4*pi*(diam1/2)^4; % Inertia for a small cylindrical plate
BB1 = inert1*E1*damp_end; % Bending Stiffness

% Segment 4 (Right Side MASS)
E4 = E1; % Young's Modulus
mu4 = mu1; % Mass/unit length
diam4 = diam1; % Side Diameter
inert4 = 1/4*pi*(diam4/2)^4; % Inertia for a small cylindrical plate
BB4 = inert4*E4*damp_end; % Bending Stiffness

%%%%%%%%%%%%%%%%%%%%%%%%%%%%%%%%%%%%%%%%%%%%%%%%%%%%%%%%%%%%%%%%%%%%%%%%

% Excitation Properties
x_ex = 0.13; % Point of excitation

load sample_info.mat % T N dt Fs
% Create frequency dependent excitation force and frequency vector

om = 2*pi*linspace(0,Fs/2,N/2+1);
freq = om/2/pi;
F_ex = ones(1,N/2+1);
F_ex(1)=0;

%%%%%%%%%%%%%%%%%%%%%%%%%%%%%%%%%%%%%%%%%%%%%%%%%%%%%%%%%%%%%%%%%%%%%%%%
% Wave numbers
% Segment 2 and 3 (String)
k_a23 = -j*sqrt(-T23/2/BB23+sqrt(T23^2/4/BB23^2+om.^2*mu23/BB23));
k_c23 = -sqrt(T23/2/BB23+sqrt(T23^2/4/BB23^2+om.^2*mu23/BB23));
k_b23 = -k_a23;

```

```

k_d23 = -k_c23;
% Segment 1 (Left Side)
k_a1 = -j*sqrt(-T14/2/BB1+sqrt(T14^2/4/BB1^2+om.^2*mu1/BB1));
k_c1 = -sqrt(T14/2/BB1+sqrt(T14^2/4/BB1^2+om.^2*mu1/BB1));
k_b1 = -k_a1;
k_d1 = -k_c1;
% Segment 4 (Right Side)
k_a4 = -j*sqrt(-T14/2/BB4+sqrt(T14^2/4/BB4^2+om.^2*mu4/BB4));
k_c4 = -sqrt(T14/2/BB4+sqrt(T14^2/4/BB4^2+om.^2*mu4/BB4));
k_b4 = -k_a4;
k_d4 = -k_c4;

%%%%%%%%%%%%%%%%%%%%%%%%%%%%%%%%%%%%%%%%%%%%%%%%%%%%%%%%%%%%%%%%%%%%%%%%%%%%%%
%%%%%%%%%%%%%%%%%%%%%%%%%%%%%%%%%%%%%%%%%%%%%%%%%%%%%%%%%%%%%%%%%%%%%%%%%%%%%%

% X = 0 at junction between sections 1 and 2 (string and left end)
% Negative to the left of that, and positive to the right
% -----|-----|-----
% <-- L/2 |-----*-----| L/2 -->
% -----|-----!-----|-----
%           x=0           x=excitation point           x=L

% All right going nearfields in section 1 are
% multiplied by exp(-k_c23(mmm)*(-del_end))
% All left going nearfields in section 2 are
% multiplied by exp(-k_d23(mmm)*x_ex)
% All left going nearfields in section 3 are
% multiplied by exp(-k_d23(mmm)*L)
% All left going nearfields in section 4 are
% multiplied by exp(-k_d23(mmm)*(L+del_end))
% This is to prevent an infinite approaching number in the left-going
% near field
% This will change the equation for our response. The response is now:
% Xi_om =
% A1*exp(k_a1*x)+B1*exp(k_b1*x)+...
% C1*exp(k_c1*(x+del_end))+D1*exp(k_d1*x)
% + A2*exp(k_a23*x)+B2*exp(k_b23*x)+...
% C2*exp(k_c23*x)+D2_prime*exp(k_d23*(x-x_ex))
% + A3*exp(k_a3*x)+B3*exp(k_b3*x)+...
% C3*exp(k_c3*x)+D3_prime*exp(k_d3*(x-L))
% + A4*exp(k_a4*x)+B4*exp(k_b4*x)+...
% C4*exp(k_c4*x)+D4_prime*exp(k_d4*(x-(L+del_end)))
% This will also change the coefficients for these special cases as well.
% C1_prime, D2_prime, D3_prime, D4_prime are:

```

```

% C1/exp(-k_c1*del_end), D2/exp(-k_d23*x_ex) and,
% D3/exp(k_d23*L), and D4/exp(k_d4*(L+del_end)) respectively
del_end = L/2;

% Allocate space for coefficients
coeff_mat = zeros(16,length(om));
for mmm = 2:N/2+1,

    left_mat = ...
        [...
        % (1)
        % BC: Disp = 0 for left side of left beam end
        exp(k_a1(mmm)*(-del_end)) ...
        exp(k_b1(mmm)*(-del_end)) ...
        exp(k_c1(mmm)*(-del_end-(-del_end))) ...
        exp(k_d1(mmm)*(-del_end)) ...
        0 0 0 0 0 0 0 0 0 0 0;...

        % (2)
        % BC: Bending angle = zero for left side of left beam end
        k_a1(mmm)*exp(k_a1(mmm)*(-del_end)) ...
        k_b1(mmm)*exp(k_b1(mmm)*(-del_end)) ...
        k_c1(mmm)*exp(k_c1(mmm)*(-del_end-(-del_end))) ...
        k_d1(mmm)*exp(k_d1(mmm)*(-del_end)) ...
        0 0 0 0 0 0 0 0 0 0 0;...

        % (3)
        % BC: Disp is same for left part of string and left beam end
        1 1 exp(-k_c1(mmm)*(-del_end)) 1 ...
        -1 -1 -1 -1*exp(-k_d23(mmm)*x_ex) ...
        0 0 0 0 0 0 0 0;...

        % (4)
        % BC: Bending angle is same for left string part and left beam end
        k_a1(mmm) k_b1(mmm) ...
        k_c1(mmm)*exp(-k_c1(mmm)*(-del_end)) k_d1(mmm) ...
        -k_a23(mmm) -k_b23(mmm) ....
        -k_c23(mmm) -k_d23(mmm)*exp(-k_d23(mmm)*x_ex) ...
        0 0 0 0 0 0 0 0;...

        % (5)
        % BC: Moment is same for left string part and left beam end
        (-BB1*k_a1(mmm)^2+T14) ...
        (-BB1*k_b1(mmm)^2+T14) ...

```

```

(-BB1*k_c1(mmm)^2+T14)*exp(-k_c1(mmm)*(-del_end)) ...
(-BB1*k_d1(mmm)^2+T14) ...
-(-BB23*k_a23(mmm)^2+T23) ...
-(-BB23*k_b23(mmm)^2+T23) ...
-(-BB23*k_c23(mmm)^2+T23) ...
-(-BB23*k_d23(mmm)^2+T23)*exp(-k_d23(mmm)*x_ex) ...
0 0 0 0 0 0 0;...

% (6)
% BC: Force is same for left string part and left beam end
(BB1*k_a1(mmm)^3+T14*k_a1(mmm)) ...
(BB1*k_b1(mmm)^3+T14*k_b1(mmm)) ...
(BB1*k_c1(mmm)^3+T14*k_c1(mmm))*exp(-k_c1(mmm)*(-del_end)) ...
(BB1*k_d1(mmm)^3+T14*k_d1(mmm)) ...
-(BB23*k_a23(mmm)^3+T23*k_a23(mmm)) ...
-(BB23*k_b23(mmm)^3+T23*k_b23(mmm)) ...
-(BB23*k_c23(mmm)^3+T23*k_c23(mmm)) ...
-(BB23*k_d23(mmm)^3+T23*k_d23(mmm))*exp(-k_d23(mmm)*x_ex) ...
0 0 0 0 0 0 0;...

% (7)
% BC: Disp is same for both string parts at string junction
0 0 0 0 ...
exp(k_a23(mmm)*x_ex) exp(k_b23(mmm)*x_ex) ...
exp(k_c23(mmm)*x_ex) exp(k_d23(mmm)*(x_ex-x_ex)) ...
-exp(k_a23(mmm)*x_ex) -exp(k_b23(mmm)*x_ex) ...
-exp(k_c23(mmm)*x_ex) -exp(k_d23(mmm)*(x_ex-L)) ...
0 0 0 0;...

% (8)
% BC: Bending angle is same for both string parts @ string junction
0 0 0 0 ...
k_a23(mmm)*exp(k_a23(mmm)*x_ex) ...
k_b23(mmm)*exp(k_b23(mmm)*x_ex) ...
k_c23(mmm)*exp(k_c23(mmm)*x_ex) ...
k_d23(mmm)*exp(k_d23(mmm)*(x_ex-x_ex)) ...
-k_a23(mmm)*exp(k_a23(mmm)*x_ex) ...
-k_b23(mmm)*exp(k_b23(mmm)*x_ex) ...
-k_c23(mmm)*exp(k_c23(mmm)*x_ex) ...
-k_d23(mmm)*exp(k_d23(mmm)*(x_ex-L)) ...
0 0 0 0;...

% (9)
% BC: Moment is same for both string parts at string junction

```



```

0 0 0 0 ...
(-BB23*k_a23(mmm)^2+T23)*exp(k_a23(mmm)*x_ex) ...
(-BB23*k_b23(mmm)^2+T23)*exp(k_b23(mmm)*x_ex) ...
(-BB23*k_c23(mmm)^2+T23)*exp(k_c23(mmm)*x_ex) ...
(-BB23*k_d23(mmm)^2+T23)*exp(k_d23(mmm)*(x_ex-x_ex)) ...
-(-BB23*k_a23(mmm)^2+T23)*exp(k_a23(mmm)*x_ex) ...
-(-BB23*k_b23(mmm)^2+T23)*exp(k_b23(mmm)*x_ex) ...
-(-BB23*k_c23(mmm)^2+T23)*exp(k_c23(mmm)*x_ex) ...
-(-BB23*k_d23(mmm)^2+T23)*exp(k_d23(mmm)*(x_ex-L)) ...
0 0 0 0;...

% (10)
% BC: Force is same for both string parts at string junction
0 0 0 0 ...
(BB23*k_a23(mmm)^3+T23*k_a23(mmm))*exp(k_a23(mmm)*x_ex) ...
(BB23*k_b23(mmm)^3+T23*k_b23(mmm))*exp(k_b23(mmm)*x_ex) ...
(BB23*k_c23(mmm)^3+T23*k_c23(mmm))*exp(k_c23(mmm)*x_ex) ...
(BB23*k_d23(mmm)^3+T23*k_d23(mmm))*exp(k_d23(mmm)*(x_ex-x_ex)) ...
-(BB23*k_a23(mmm)^3+T23*k_a23(mmm))*exp(k_a23(mmm)*x_ex) ...
-(BB23*k_b23(mmm)^3+T23*k_b23(mmm))*exp(k_b23(mmm)*x_ex) ...
-(BB23*k_c23(mmm)^3+T23*k_c23(mmm))*exp(k_c23(mmm)*x_ex) ...
-(BB23*k_d23(mmm)^3+T23*k_d23(mmm))*exp(k_d23(mmm)*(x_ex-L)) ...
0 0 0 0;...

% (11)
% BC: Disp is same for right string part and right beam end
0 0 0 0 0 0 0 0 ...
exp(k_a23(mmm)*L) exp(k_b23(mmm)*L) ...
exp(k_c23(mmm)*L) exp(k_d23(mmm)*(L-L)) ...
-exp(k_a4(mmm)*L) -exp(k_b4(mmm)*L) ...
-exp(k_c4(mmm)*L) -exp(k_d4(mmm)*(L-(L+del_end)));...

% (12)
% BC: Bending angle is same at right string part and right beam end
0 0 0 0 0 0 0 0 ...
k_a23(mmm)*exp(k_a23(mmm)*L) ...
k_b23(mmm)*exp(k_b23(mmm)*L) ...
k_c23(mmm)*exp(k_c23(mmm)*L) ...
k_d23(mmm)*exp(k_d23(mmm)*(L-L)) ...
-k_a4(mmm)*exp(k_a4(mmm)*L) ...
-k_b4(mmm)*exp(k_b4(mmm)*L) ...
-k_c4(mmm)*exp(k_c4(mmm)*L) ...
-k_d4(mmm)*exp(k_d4(mmm)*(L-(L+del_end))); ...

```

```

% (13)
% BC: Moment is same for right string part and right beam end
0 0 0 0 0 0 0 0 ...
(-BB23*k_a23(mmm)^2+T23)*exp(k_a23(mmm)*L) ...
(-BB23*k_b23(mmm)^2+T23)*exp(k_b23(mmm)*L) ...
(-BB23*k_c23(mmm)^2+T23)*exp(k_c23(mmm)*L) ...
(-BB23*k_d23(mmm)^2+T23)*exp(k_d23(mmm)*(L-L)) ...
-(-BB4*k_a4(mmm)^2+T14)*exp(k_a4(mmm)*L) ...
-(-BB4*k_b4(mmm)^2+T14)*exp(k_b4(mmm)*L) ...
-(-BB4*k_c4(mmm)^2+T14)*exp(k_c4(mmm)*L) ...
-(-BB4*k_d4(mmm)^2+T14)*exp(k_d4(mmm)*(L-(L+del_end))); ...

% (14)
% BC: Force is same for right string part and right beam end
0 0 0 0 0 0 0 0 ...
(BB23*k_a23(mmm)^3+T23*k_a23(mmm))*exp(k_a23(mmm)*L) ...
(BB23*k_b23(mmm)^3+T23*k_b23(mmm))*exp(k_b23(mmm)*L) ...
(BB23*k_c23(mmm)^3+T23*k_c23(mmm))*exp(k_c23(mmm)*L) ...
(BB23*k_d23(mmm)^3+T23*k_d23(mmm))*exp(k_d23(mmm)*(L-L)) ...
- (BB4*k_a4(mmm)^3+T14*k_a4(mmm))*exp(k_a4(mmm)*L) ...
- (BB4*k_b4(mmm)^3+T14*k_b4(mmm))*exp(k_b4(mmm)*L) ...
- (BB4*k_c4(mmm)^3+T14*k_c4(mmm))*exp(k_c4(mmm)*L) ...
- (BB4*k_d4(mmm)^3+T14*k_d4(mmm))*exp(k_d4(mmm)*(L-(L+del_end)));...

% (15)
% BC: Disp = 0 for right side of right beam end
0 0 0 0 0 0 0 0 0 0 0 0 ...
exp(k_a4(mmm)*(L+del_end)) ...
exp(k_b4(mmm)*(L+del_end)) ...
exp(k_c4(mmm)*(L+del_end)) ...
exp(k_d4(mmm)*(L+del_end-(L+del_end)));...

% (16)
% BC: Bending angle = zero for right side of right beam end
0 0 0 0 0 0 0 0 0 0 0 0 ...
k_a4(mmm)*exp(k_a4(mmm)*(L+del_end)) ...
k_b4(mmm)*exp(k_b4(mmm)*(L+del_end)) ...
k_c4(mmm)*exp(k_c4(mmm)*(L+del_end)) ...
k_d4(mmm)*exp(k_d4(mmm)*(L+del_end-(L+del_end)));...
];

right_mat = [...
0; 0; ...
0; 0; 0; 0; ...

```

```

    0; 0; 0; -F_ex(mmm); ...
    0; 0; 0; 0; ...
    0; 0];

%   coeff_mat = [A1; B1; C1; D1; A2; B2; C2; D2_prime;...
%               A3; B3; C3; D3_prime; A4; B4; C4; D4_prime];
    coeff_mat(:,mmm) = left_mat\right_mat;

end

% A1 = coeff_mat(1,:); B1 = coeff_mat(2,:);
% C1 = coeff_mat(3,:); D1 = coeff_mat(4,:);
% A2 = coeff_mat(5,:); B2 = coeff_mat(6,:);
% C2 = coeff_mat(7,:); D2 = coeff_mat(8,:);
% A3 = coeff_mat(9,:); B3 = coeff_mat(10,:);
% C3 = coeff_mat(11,:); D3 = coeff_mat(12,:);
% A4 = coeff_mat(13,:); B4 = coeff_mat(14,:);
% C4 = coeff_mat(15,:); D4 = coeff_mat(16,:);
%%%%%%%%%%%%%%%%%%%%%%%%%%%%%%%%%%%%%%%%%%%%%%%%%%%%%%%%%%%%%%%%%%%%%%%%

save wave_coeff.mat om freq L x_ex coeff_mat k_* E23 diam23 mu23
save wave_force F_ex
warning('on')

```

B.2 Input Force

```

% This workspace will determine what force is input into the string for the
% remainder of the calculations. This does not take into account the
% reponse of the string, but does make the final contact point of plectrum
% and string to be a specific displacement

% load str_displace.mat C_length % str_disp total_disp C_length str_acc
C_length = 512;
tt = linspace(0,1,C_length);
Fs = 51200;
N = 131072;
T = 2.56;
dt = T/N;
t=linspace(0,T,N);
freq = linspace(0,Fs/2,N/2+1);
om = linspace(0,Fs,N)*2*pi;

```

```

load string_prop.mat T23 % load the Tension
load wave_coeff.mat x_ex L % load the excitation point and string length

% F_ex = tt.^2;
F_ex = real(T23)*...
    [sin(tan(0.1*t(1:C_length)/x_ex)) + ...
     sin(tan(0.1*t(1:C_length)/(L-x_ex)))];
% F_ex = 1;

load point_compliance.mat
Xi_PC_IR = ifft(Xi_PC_FR);
str_resp = conv(Xi_PC_IR,F_ex);
F_scale = 0.001/max(abs(str_resp));
F_ex = F_ex*F_scale;
save force_input.mat F_ex N C_length
save sample_info.mat T N dt Fs

```

B.3 Bridge Acceleration

% This workspace will calculate the transversal wave bridge acceleration
 % using finite difference approximations. These bridge accelerations will be
 % used to compare with the measured bridge accelerations.

```

load sample_info.mat % T N dt Fs
t = linspace(0,T,N);
load string_prop.mat % BB23 T23 (Bending stiffness and Tension)
load wave_coeff.mat % om freq L x_ex coeff_mat k_* E23 diam23 F_ex
load force_input.mat % F_ex N C_length

% Using wave_coeff_calc_fix.m, which assumes the ends to be highly
% damped but fixed at some point, creates the following for the wave_coeff
% A1 = coeff_mat(1,:); B1 = coeff_mat(2,:);
% C1 = coeff_mat(3,:); D1 = coeff_mat(4,:);
  A2 = coeff_mat(5,:); B2 = coeff_mat(6,:);
  C2 = coeff_mat(7,:); D2 = coeff_mat(8,:);
  A3 = coeff_mat(9,:); B3 = coeff_mat(10,:);
  C3 = coeff_mat(11,:); D3 = coeff_mat(12,:);
% A4 = coeff_mat(13,:); B4 = coeff_mat(14,:);
% C4 = coeff_mat(15,:); D4 = coeff_mat(16,:);

clear coeff_mat

```

```

% Retrieve the displacement and transfer it into the time domain
disp_bridge_sim = zeros(1,N+length(F_ex)-1);
disp_bridge_sim(1:N/2+1) = A3.*exp(k_a23.*L) + B3.*exp(k_b23.*L) + ...
    C3.*exp(k_c23.*L) + D3.*exp(k_d23.*(L-L));
disp_bridge_sim(N/2+2:N)=fliplr(conj(disp_bridge_sim(2:N/2)));
disp_bridge_sim(N/2+1)=real(disp_bridge_sim(N/2+1));
disp_bridge_sim = conv(iffit(disp_bridge_sim(1:N)),F_ex);
disp_bridge_sim = disp_bridge_sim(1:N);

% Calculate the bridge acceleration using difference approximations
acc_bridge_sim = zeros(1,N);
acc_bridge_sim(1) = [2*disp_bridge_sim(1) - 5*disp_bridge_sim(2) + ...
    4*disp_bridge_sim(3) - 1*disp_bridge_sim(4)]/2/dt;
for aa = 2:N-1,
    acc_bridge_sim(aa) = [disp_bridge_sim(aa-1) - ...
        2*disp_bridge_sim(aa) + 1*disp_bridge_sim(aa+1)]/2/dt;
end
acc_bridge_sim(N) = [-1*disp_bridge_sim(N-3) + 4*disp_bridge_sim(N-2) - ...
    5*disp_bridge_sim(N-1) + 2*disp_bridge_sim(N)]/2/dt;

```

B.4 Longitudinal Displacement - Part 1

```

% This workspace will calculate the coupling force of transversal to
% longitudinal waves using a finite difference method. The string is broken
% up into sections, and the sections are then grouped together to reduce
% the computation time required.
% This computation is derived from the method explained in Bank and
% Sujbert's paper "Generation of longitudinal vibration in piano strings:
% From physics to sound synthesis
home

disp('Beginning of operations')
klockan = clock; disp(horzcat(num2str(klockan(4)),...
    ':' ,int2str(floor(klockan(5)/10)), ...
    num2str(mod(klockan(5),10)+.01*klockan(6)))), disp(' '))

clear all
tic
% wave_and_coeff.m calculates variables for this workspace

load string_prop.mat % BB23 T23 rho23
load sample_info.mat % T N dt Fs

```

```

t = linspace(0,T,N);
load wave_coeff.mat % om freq L x_ex coeff_mat k_* E23 diam23 mu23 F_ex
load force_input.mat % F_ex C_length
% This is for the wave equations:
% Xi1_om = A1*exp(k_a1*x)+B1*exp(k_b1*x) + ...
%           C1_prime*exp(k_c1*(x+del_end))+D1*exp(k_d1*x)
% Xi2_om = A2*exp(k_a23*x)+B2*exp(k_b23*x) + ...
%           C2*exp(k_c23*x)+D2_prime*exp(k_d23*(x-x_ex))
% Xi3_om = A3*exp(k_a23*x)+B3*exp(k_b23*x) + ...
%           C3*exp(k_c23*x)+D3_prime*exp(k_d23*(x-L))
% Xi4_om = A4*exp(k_a4*x)+B4*exp(k_b4*x) + ...
%           C4*exp(k_c4*x)+D4_prime*exp(k_d4*(x-(L+del_end)))

% Using wave_coeff_calc_fix.m, which assumes the ends to be highly
% damped but fixed at some point, creates the following for the wave_coeff
% A1 = coeff_mat(1,:); B1 = coeff_mat(2,:);
% C1 = coeff_mat(3,:); D1 = coeff_mat(4,:);
% A2 = coeff_mat(5,:); B2 = coeff_mat(6,:);
% C2 = coeff_mat(7,:); D2 = coeff_mat(8,:);
% A3 = coeff_mat(9,:); B3 = coeff_mat(10,:);
% C3 = coeff_mat(11,:); D3 = coeff_mat(12,:);
% A4 = coeff_mat(13,:); B4 = coeff_mat(14,:);
% C4 = coeff_mat(15,:); D4 = coeff_mat(16,:);

clear coeff_mat

%%%%%%%%%%%%%%%%%%%%%%%%%%%%%%%%%%%%%%%%%%%%%%%%%%%%%%%%%%%%%%%%%%%%%%%%
str_resolut = 10000;
xline = [0:L/str_resolut:L];
xline2 = xline(1:max(find(xline<=x_ex)));
xline3 = xline(min(find(xline>x_ex)):length(xline));

ES23 = E23*pi*(diam23/2)^2; % The term E*S (Young's * cross sec area)
c_L = sqrt(E23/rho23); % Speed of sound of longitudinal waves
n_max = floor(2*L*freq(length(freq))/c_L);
f_L = [1:n_max]*c_L/2/L; % Longitudinal frequencies
k = [1:1:n_max]'; % Number of modes of longitudinal waves

% Force coupling from transversal to longitudinal waves
F_Trans_to_Long = zeros(n_max,2*length(om)-2);

%%%%%%%%%%%%%%%%%%%%%%%%%%%%%%%%%%%%%%%%%%%%%%%%%%%%%%%%%%%%%%%%%%%%%%%%
disp('Perform the first loop outside of the loop because of the boundary')
klockan = clock; disp(horzcat(num2str(klockan(4)),...

```

```

    ',int2str(floor(klockan(5)/10)), ...
    num2str(mod(klockan(5),10)+.01*klockan(6))), disp(' ')
%%%%%%%%%%%%%%%%%%%%%%%%%%%%%%%%%%%%%%%%%%%%%%%%%%%%%%%%%%%%%%%%%%%%%%%%
% Perform the first loop outside of the loop because of the boundary
L_sec = 4; % Take this many points of the string at a time
L_FR = length(t)/2;
Xi_FR = zeros(L_sec,length(t));
Xi_IR = zeros(L_sec+3,length(t));
Xi_IR_dum = zeros(1,length(t)+C_length-1);
Xi_IR_prime_sq = zeros(L_sec+2,length(t));
xline_part = zeros(1,L_sec+3); % The +3 are values to be carried over
xline_part(1:4) = xline2(1:4);

Xi_FR(1:4,1:L_FR+1) = [...
    A2'*ones(1,4).*exp(k_a23'*xline_part(1:4)) + ...
    B2'*ones(1,4).*exp(k_b23'*xline_part(1:4)) + ...
    C2'*ones(1,4).*exp(k_c23'*xline_part(1:4)) + ...
    D2'*ones(1,4).*exp(k_d23'*(xline_part(1:4)-x_ex*ones(1,4)))]';

Xi_FR(1:4,L_FR+2:2*L_FR) = fliplr(conj(Xi_FR(1:4,2:L_FR)));
Xi_FR(1:4,L_FR+1) = real(Xi_FR(1:4,L_FR+1));
Xi_IR(1:4) = ifft(Xi_FR(1:4), [], 2);
for dd=1:4, % Convolute the compliance with the Input Force
    Xi_IR_dum = conv(Xi_IR(dd,:),F_ex);
    Xi_IR(dd,:) = Xi_IR_dum(1:N);
end

% Calculate the Trans to Long force at first point (left boundary)
Xi_IR_prime_sq(1,:) = [...
    (-3*Xi_IR(1,:) + 4*Xi_IR(2,:) - Xi_IR(3,:))/(2*L/str_resolut)...
    ].^2;
Xi_IR_prime_sq(2,:) = [...
    (Xi_IR(3,:) - Xi_IR(1,:))/(2*L/str_resolut)...
    ].^2;
Xi_IR_prime_sq(3,:) = [...
    (Xi_IR(4,:) - Xi_IR(2,:))/(2*L/str_resolut)...
    ].^2;
% Coupled force from point 1 of length(xline)
F_Trans_to_Long = F_Trans_to_Long + [sin(k*pi*xline_part(1)/L)*...
    (-3*Xi_IR_prime_sq(1,:) + 4*Xi_IR_prime_sq(2,:) - ...
    Xi_IR_prime_sq(3,:))/(2*L/str_resolut)]*(L/str_resolut);
% Coupled force from point 2 of length(xline)
F_Trans_to_Long = F_Trans_to_Long + [sin(k*pi*xline_part(2)/L)*...
    (Xi_IR_prime_sq(3,:)-Xi_IR_prime_sq(1)) / ...

```

```

(2*L/str_resolut)]*(L/str_resolut);

% END of first calculation outside of the loop because of the boundary
%%%%%%%%%%%%%%%%%%%%%%%%%%%%%%%%%%%%%%%%%%%%%%%%%%%%%%%%%%%%%%%%%%%%%%%%
Xi_dummy_1 = Xi_IR(2,:);
Xi_dummy_2 = Xi_IR(3,:);
Xi_dummy_3 = Xi_IR(4,:);
Xi_dummy_prime_1 = Xi_IR_prime_sq(2,:);
Xi_dummy_prime_2 = Xi_IR_prime_sq(3,:);
xline_part(end-2:end) = xline_part(2:4);
%%%%%%%%%%%%%%%%%%%%%%%%%%%%%%%%%%%%%%%%%%%%%%%%%%%%%%%%%%%%%%%%%%%%%%%%
disp('Beginning of loop for remain of section 2 (left part of string)')
klockan = clock; disp(horzcat(num2str(klockan(4)),...
    ', ',int2str(floor(klockan(5)/10)), ...
    num2str(mod(klockan(5),10)+.01*klockan(6))))), disp(' ')
%%%%%%%%%%%%%%%%%%%%%%%%%%%%%%%%%%%%%%%%%%%%%%%%%%%%%%%%%%%%%%%%%%%%%%%%
% Beginning of loop for remain of section 2 (left part of string)

Xi_FR = zeros(L_sec,length(t));
Xi_IR = zeros(L_sec+3,length(t));
Xi_IR_prime_sq = zeros(L_sec+2,length(t));
Xi_IR(end-2,:) = Xi_dummy_1; % To help carry over to loops
Xi_IR(end-1,:) = Xi_dummy_2; % To help carry over to loops
Xi_IR(end,:) = Xi_dummy_3; % To help carry over to loops
Xi_IR_prime_sq(end-1,:) = Xi_dummy_prime_1; % To help carry over to loops
Xi_IR_prime_sq(end,:) = Xi_dummy_prime_2; % To help carry over to loops

% Number of times to loop through section 2 before moving on to section 3
num_loops2 = floor((length(xline2)-4)/L_sec);
% The remaining part of section 2 that will need to be included in the
% combined calculation of sections 2 and 3
remain_part2 = length(xline2(2:end))-L_sec*num_loops2;

for gg=1:num_loops2,
% Not Needed % Xi_IR(1,:) = Xi_IR(end-2,:); % Carryover from prev loop
    Xi_IR(2,:) = Xi_IR(end-1,:); % Carryover from prev loop
    Xi_IR(3,:) = Xi_IR(end,:); % Carryover from prev loop
    Xi_IR_prime_sq(1,:) = Xi_IR_prime_sq(end-1,:); % Carryover from loop
    Xi_IR_prime_sq(2,:) = Xi_IR_prime_sq(end,:); % Carryover from loop
    xline_part(1:3) = xline_part(end-2:end);

    % Create vector of "L_sec" locations of the string
    % Length consists of 1(carry over to left), Lsec, 2(to right)
    xline_part(4:end) = xline2( L_sec*(gg-1)+5 : L_sec*gg+4 );

```



```

Xi_FR(:,1:L_FR+1) = [...
    A2'*ones(1,L_sec).*exp(k_a23'*xline_part(4:end)) + ...
    B2'*ones(1,L_sec).*exp(k_b23'*xline_part(4:end)) + ...
    C2'*ones(1,L_sec).*exp(k_c23'*xline_part(4:end)) + ...
    D2'*ones(1,L_sec).*...
    exp(k_d23'*(xline_part(4:end)-x_ex*ones(1,L_sec)))]';

Xi_FR(:,L_FR+2:2*L_FR) = fliplr(conj(Xi_FR(:,2:L_FR)));
Xi_FR(:,L_FR+1) = real(Xi_FR(:,L_FR+1));
Xi_IR(4:L_sec+3,:) = ifft(Xi_FR,[],2);
for dd=4:L_sec+3, % Convolute the compliance with the Input Force
    Xi_IR_dum = conv(Xi_IR(dd,:),F_ex);
    Xi_IR(dd,:) = Xi_IR_dum(1:N);
end

for pp=1:L_sec,
    Xi_IR_prime_sq(pp+2,:) = ...
        [(Xi_IR(pp+3,:) - Xi_IR(pp+1,:))/(2*L/str_resolut)].^2;
    F_Trans_to_Long = F_Trans_to_Long + ...
        [sin(k*pi*xline_part(pp+1)/L) *...
        (Xi_IR_prime_sq(pp+2,)-Xi_IR_prime_sq(pp,:)) / ...
        (2*L/str_resolut)]*(L/str_resolut);
end
end

% End of loop for remain of section 2 (left part of string)
%%%%%%%%%%%%%%%%%%%%%%%%%%%%%%%%%%%%%%%%%%%%%%%%%%%%%%%%%%%%%%%%%%%%%%%%
% Not Needed % Xi_IR(1,:) = Xi_IR(end-2,:); % Carryover from loop
Xi_IR(2,:) = Xi_IR(end-1,:); % Carryover from loop
Xi_IR(3,:) = Xi_IR(end,:); % Carryover from loop
Xi_IR_prime_sq(1,:) = Xi_IR_prime_sq(end-1,:); % Carryover from loop
Xi_IR_prime_sq(2,:) = Xi_IR_prime_sq(end,:); % Carryover from loop
xline_part(1:3) = xline_part(end-2:end);
%%%%%%%%%%%%%%%%%%%%%%%%%%%%%%%%%%%%%%%%%%%%%%%%%%%%%%%%%%%%%%%%%%%%%%%%
disp('Portion of string that is shared by both sections 2 and 3')
klockan = clock; disp(horzcat(num2str(klockan(4)),...
    ':',int2str(floor(klockan(5)/10)), ...
    num2str(mod(klockan(5),10)+.01*klockan(6))), disp(' '))
%%%%%%%%%%%%%%%%%%%%%%%%%%%%%%%%%%%%%%%%%%%%%%%%%%%%%%%%%%%%%%%%%%%%%%%%
% Portion of string that is shared by both sections 2 and 3

% Create vector for "L_sec" locations of the string
% Length consists of 1(carry over to left), Lsec, 2(to right)

```

```

xline_part(4:end) = horzcat(...
    xline2( end-remain_part2+4 : end ) , ...
    xline3(1:L_sec+3-remain_part2));
% xline_test(aaaa,:) = xline_part; aaaa = aaaa+1;

% Calculate the FR of the parts of section two that have not been
% calculated yet. ie. at least 3 parts from section 2 will be carried over,
% so this will calculate the remaining parts
Xi_FR(1:remain_part2-3,1:L_FR+1) = [...
    A2'*ones(1,remain_part2-3).*...
        exp(k_a23*xline_part(4:remain_part2)) + ...
    B2'*ones(1,remain_part2-3).*...
        exp(k_b23*xline_part(4:remain_part2)) + ...
    C2'*ones(1,remain_part2-3).*...
        exp(k_c23*xline_part(4:remain_part2)) + ...
    D2'*ones(1,remain_part2-3).* ...
        exp(k_d23*(xline_part(4:remain_part2)-x_ex*ones(1,remain_part2-3)))]';

Xi_FR(remain_part2-3+1:end,1:L_FR+1) = [...
    A3'*ones(1,L_sec-remain_part2+3).*...
        exp(k_a23*xline_part(remain_part2+1:end)) + ...
    B3'*ones(1,L_sec-remain_part2+3).*...
        exp(k_b23*xline_part(remain_part2+1:end)) + ...
    C3'*ones(1,L_sec-remain_part2+3).*...
        exp(k_c23*xline_part(remain_part2+1:end)) + ...
    D3'*ones(1,L_sec-remain_part2+3).* ...
        exp(k_d23*(xline_part(remain_part2+1:end)-...
            L*ones(1,L_sec-remain_part2+3)))]';

Xi_FR(:,L_FR+2:2*L_FR) = fliplr(conj(Xi_FR(:,2:L_FR)));
Xi_FR(:,L_FR+1) = real(Xi_FR(:,L_FR+1));
Xi_IR(4:L_sec+3,:) = ifft(Xi_FR,[],2);
for dd=4:L_sec+3, % Convolute the compliance with the Input Force
    Xi_IR_dum = conv(Xi_IR(dd,:),F_ex);
    Xi_IR(dd,:) = Xi_IR_dum(1:N);
end

for pp=1:L_sec,
    Xi_IR_prime_sq(pp+2,:) = ...
        [(Xi_IR(pp+3,:) - Xi_IR(pp+1,:))/(2*L/str_resolut)].^2;
    F_Trans_to_Long = F_Trans_to_Long + ...
        [sin(k*pi*xline_part(pp+1)/L) *...
        (Xi_IR_prime_sq(pp+2,)-Xi_IR_prime_sq(pp,:)) / ...
        (2*L/str_resolut)]*(L/str_resolut);

```

```

end

% End of Portion of string that is shared by both sections 2 and 3
%%%%%%%%%%%%%%%%%%%%%%%%%%%%%%%%%%%%%%%%%%%%%%%%%%%%%%%%%%%%%%%%%%%%%%%%
disp('Beginning of loop portion for section 3 (Right Part of String)')
klockan = clock; disp(horzcat(num2str(klockan(4)),...
    ':',int2str(floor(klockan(5)/10)), ...
    num2str(mod(klockan(5),10)+.01*klockan(6))), disp(' '))
%%%%%%%%%%%%%%%%%%%%%%%%%%%%%%%%%%%%%%%%%%%%%%%%%%%%%%%%%%%%%%%%%%%%%%%%
% Beginning of loop portion for section 3 (Right Part of String)

% Number of times to loop through section 3 before managing with the end
% boundary problem situation
num_loops3 = floor((length(xline3)-(L_sec+3-remain_part2))/L_sec);
% The remaining part of section 3 that will need to be included when
% calculating the right boundary of section 3
remain_part3 = length(xline3)-(L_sec-remain_part2)-num_loops3*L_sec;

for gg=1:num_loops3,
% Not Needed % Xi_IR(1,:) = Xi_IR(end-2,:); % Carryover from prev loop
    Xi_IR(2,:) = Xi_IR(end-1,:); % Carryover from prev loop
    Xi_IR(3,:) = Xi_IR(end,:); % Carryover from prev loop
    Xi_IR_prime_sq(1,:) = Xi_IR_prime_sq(end-1,:); % Carryover from loop
    Xi_IR_prime_sq(2,:) = Xi_IR_prime_sq(end,:); % Carryover from loop
    xline_part(1:3) = xline_part(end-2:end);

    % Create vector of "L_sec" locations of the string
    % Length consists of 1(carry over to left), Lsec, 2(to right)
    xline_part(4:end) = ...
        xline3( L_sec*gg-remain_part2+4 : L_sec*(gg+1)-remain_part2+3 );
%    xline_test(aaaa,:) = xline_part; aaaa = aaaa+1;

    Xi_FR(:,1:L_FR+1) = [...
        A3'*ones(1,L_sec).*exp(k_a23'*xline_part(4:end)) + ...
        B3'*ones(1,L_sec).*exp(k_b23'*xline_part(4:end)) + ...
        C3'*ones(1,L_sec).*exp(k_c23'*xline_part(4:end)) + ...
        D3'*ones(1,L_sec).*...
        exp(k_d23'*(xline_part(4:end)-L*ones(1,L_sec)))]';

    Xi_FR(:,L_FR+2:2*L_FR) = fliplr(conj(Xi_FR(:,2:L_FR)));
    Xi_FR(:,L_FR+1) = real(Xi_FR(:,L_FR+1));
    Xi_IR(4:L_sec+3,:) = ifft(Xi_FR,[],2);
    for dd=4:L_sec+3, % Convolute the compliance with the Input Force
        Xi_IR_dum = conv(Xi_IR(dd,:),F_ex);
    end
end

```

```

        Xi_IR(dd,:) = Xi_IR_dum(1:N);
    end

    for pp=1:L_sec,
        Xi_IR_prime_sq(pp+2,:) = ...
            [(Xi_IR(pp+3,:) - Xi_IR(pp+1,:))/(2*L/str_resolut)].^2;
        F_Trans_to_Long = F_Trans_to_Long + ...
            [sin(k*pi*xline_part(pp+1)/L) *...
            (Xi_IR_prime_sq(pp+2,)-Xi_IR_prime_sq(pp,:)) / ...
            (2*L/str_resolut)]*(L/str_resolut);
    end
end

% End of section 3, which is separate from section 2 and the right boundary
%%%%%%%%%%%%%%%%%%%%%%%%%%%%%%%%%%%%%%%%%%%%%%%%%%%%%%%%%%%%%%%%%%%%%%%%%%
Xi_IR(1,:) = Xi_IR(end-2,:); % Carryover from prev loop (Normally not
% needed, but used here because it will be saved for later use
Xi_IR(2,:) = Xi_IR(end-1,:); % Carryover from prev loop
Xi_IR(3,:) = Xi_IR(end,:); % Carryover from prev loop
Xi_IR_prime_sq(1,:) = Xi_IR_prime_sq(end-1,:); % Carryover from loop
Xi_IR_prime_sq(2,:) = Xi_IR_prime_sq(end,:); % Carryover from loop
xline_part(1:3) = xline_part(end-2:end);
%%%%%%%%%%%%%%%%%%%%%%%%%%%%%%%%%%%%%%%%%%%%%%%%%%%%%%%%%%%%%%%%%%%%%%%%%%
disp('Beginning of right boundary situation of section 3')
klockan = clock; disp(horzcat(num2str(klockan(4)),...
    ',' ,int2str(floor(klockan(5)/10)), ...
    num2str(mod(klockan(5),10)+.01*klockan(6)))) , disp(' '))
%%%%%%%%%%%%%%%%%%%%%%%%%%%%%%%%%%%%%%%%%%%%%%%%%%%%%%%%%%%%%%%%%%%%%%%%%%
% Beginning of right boundary situation of section 3

xline_part(4:remain_part3) = xline3(end-(remain_part3-3)+1:end);
% xline_test(aaaa,:) = xline_part; aaaa = aaaa+1;

Xi_FR(:,1:L_FR+1) = [...
    A3'*ones(1,L_sec).*exp(k_a23'*xline_part(4:end)) + ...
    B3'*ones(1,L_sec).*exp(k_b23'*xline_part(4:end)) + ...
    C3'*ones(1,L_sec).*exp(k_c23'*xline_part(4:end)) + ...
    D3'*ones(1,L_sec).*exp(k_d23'*(xline_part(4:end)-L*ones(1,L_sec)))]';

Xi_FR(:,L_FR+2:2*L_FR) = fliplr(conj(Xi_FR(:,2:L_FR)));
Xi_FR(:,L_FR+1) = real(Xi_FR(:,L_FR+1));
Xi_IR(4:L_sec+3,:) = ifft(Xi_FR,[],2);
for dd=4:L_sec+3, % Convolute the compliance with the Input Force
    Xi_IR_dum = conv(Xi_IR(dd,:),F_ex);
end

```

```

    Xi_IR(dd,:) = Xi_IR_dum(1:N);
end

Xi_IR_bridge = Xi_IR(remain_part3-2:remain_part3,:);
xline_bridge = xline_part(remain_part3-2:remain_part3);
save trans_disp_bridge.mat Xi_IR_bridge xline_bridge str_resolut
% last 3 values of right part of string for use in calculating the
% longitudinal force into the soundboard in longitude_bridge_force.mat

for pp=1:remain_part3-3,
    Xi_IR_prime_sq(pp+2,:) = ...
        [(Xi_IR(pp+3,:) - Xi_IR(pp+1,:))/(2*L/str_resolut)].^2;
    F_Trans_to_Long = F_Trans_to_Long + ...
        [sin(k*pi*xline_part(pp+1)/L) *...
        (Xi_IR_prime_sq(pp+2,)-Xi_IR_prime_sq(pp,:)) / ...
        (2*L/str_resolut)]*(L/str_resolut);
end

% Calculate the Trans to Long force at last point (Right boundary)
Xi_IR_prime_sq(remain_part3-1,:) = [...
    (Xi_IR(remain_part3-2,:) - Xi_IR(remain_part3,:))/...
    (2*L/str_resolut)...
    ].^2;
Xi_IR_prime_sq(remain_part3,:) = [...
    (-3*Xi_IR(remain_part3,:) + ...
    4*Xi_IR(remain_part3-1,:) - ...
    Xi_IR(remain_part3-2,:))/(2*L/str_resolut)...
    ].^2;
% Coupled force from end point-1 of length(xline)
F_Trans_to_Long = F_Trans_to_Long + ...
    [sin(k*pi*xline_part(remain_part3-1)/L)*...
    (Xi_IR_prime_sq(remain_part3-2,)-Xi_IR_prime_sq(remain_part3))/...
    (2*L/str_resolut)]*(L/str_resolut);
% Coupled force from end point of length(xline)
F_Trans_to_Long = F_Trans_to_Long + ...
    [sin(k*pi*xline_part(remain_part3)/L)*...
    (-3*Xi_IR_prime_sq(remain_part3,:) + ...
    4*Xi_IR_prime_sq(remain_part3-1,:) - ...
    Xi_IR_prime_sq(remain_part3-2,:)) / ...
    (2*L/str_resolut)]*(L/str_resolut);

F_Trans_to_Long = 1/2*ES23*F_Trans_to_Long;

% To remove the tail of the time signal

```

```

fonstret = hanning(40,'periodic');
fonstret = ones(n_max,1)*fliplr(fonstret(1:21));
F_Trans_to_Long(:,end-20:end) = F_Trans_to_Long(:,end-20:end).*fonstret;

save Force.mat F_Trans_to_Long str_resolut

%%%%%%%%%%%%%%%%%%%%%%%%%%%%%%%%%%%%%%%%%%%%%%%%%%%%%%%%%%%%%%%%%%%%%%%%
disp('End of operations')
klockan = clock; disp(horzcat(num2str(klockan(4)),...
    ':',int2str(floor(klockan(5)/10)), ...
    num2str(mod(klockan(5),10)+.01*klockan(6))))), disp(' ')
%%%%%%%%%%%%%%%%%%%%%%%%%%%%%%%%%%%%%%%%%%%%%%%%%%%%%%%%%%%%%%%%%%%%%%%%
disp(horzcat('Total calculation took ', num2str(toc/60),' minutes'))
disp(' ')
disp('%%%%%%%%%%%%%%%%%%%%%%%%%%%%%%%%%%%%%%%%%%%%%%%%%%%%%%%%%%%%%%%%%%%%%%%%')
disp(' ')
% run longitude_disp

```

B.5 Longitudinal Displacement - Part 2

```

% This workspace will calculate the displacement vs. time at a point on the
% string. For our case, it will most likely be at the bridge, x=L.
% This computation is according to the method explained in Bank and
% Sujbert's paper "Generation of longitudinal vibration in piano strings:
% From physics to sound synthesis

```

```

disp('Beginning of convolution operations for Longitudinal displacement')
klockan = clock; disp(horzcat(num2str(klockan(4)),...
    ':',int2str(floor(klockan(5)/10)), ...
    num2str(mod(klockan(5),10)+.01*klockan(6))))), disp(' ')

home
clear all
% wave_and_coeff.m calculates variables for this workspace

load string_prop.mat % BB23 T23 rho23
load sample_info.mat % T N dt Fs
t = linspace(0,T,N);
load Force.mat % F_Trans_to_Long str_resolut
load wave_coeff.mat om freq L x_ex E23 diam23 mu23

c_L = sqrt(E23/rho23); % Speed of sound of longitudinal waves

```

CHALMERS, Master's Thesis 2007:71

```

n_max = floor(2*L*freq(end)/c_L);
f_L = [1:n_max]*c_L/2/L;
tau_L = ones(1,n_max)*0.1;

L_dummy = zeros(1,length(t));
L_dummy_sum = L_dummy;
L_disp_dum = zeros(1,2*length(t)-1);

for gg = 1:n_max,
    L_dummy = 1/pi/L/real(mu23)*...
        exp(-t./tau_L(gg))/f_L(gg).*sin(2*pi*f_L(gg)*t);
    figure(gg+200), subplot(321), plot(L_dummy)
    title('IR of Longitudinal Mode')
    xlabel('time [s]')
    figure(gg+200), subplot(322), plot(F_Trans_to_Long(gg,:))
    title('IR of Trans to Longi Force Coupling')
    xlabel('time [s]')
    pause(3)
    L_disp_dum(1,:) = conv(F_Trans_to_Long(gg,:),L_dummy);
    figure(gg+200), subplot(3,2,3:6), plot(L_disp_dum)
    disp(gg)
    L_save_name = ['L_disp_tempsave_',int2str(gg),'.mat'];
    save(L_save_name, 'L_disp_dum')
end

L_disp = zeros(n_max,2*length(t)-1);
for gg=1:n_max,
    L_save_name = ['L_disp_tempsave_',int2str(gg),'.mat'];
    load(L_save_name)
    L_disp(gg,:)=L_disp_dum;
    delete(L_save_name)
end

L_disp = L_disp(:,1:N);
save Long_displacement.mat L_disp

disp('End of operations')
klockan = clock; disp(horzcat(num2str(klockan(4)),...
    ':',int2str(floor(klockan(5)/10)), ...
    num2str(mod(klockan(5),10)+.01*klockan(6))))), disp(' ')
disp(horzcat('Total calculation took ', num2str(toc/60),' minutes'))

for gg=1:n_max,
    save_name = ['trans_to_longi_',int2str(gg),'_finediff.fig'];

```

```
saveas(figure(200+gg),save_name)
end
```

B.6 Longitudinal Bridge Force

```
% This workspace calculates the resulting force from the longitudinal
% vibrations within the string.
% This computation is according to the method explained in Bank and
% Sujbert's paper "Generation of longitudinal vibration in piano strings:
% From physics to sound synthesis

disp('Beginning of convolution operations for Longitudinal displacement')
klockan = clock; disp(horzcat(num2str(klockan(4)),...
    ':' ,int2str(floor(klockan(5)/10)), ...
    num2str(mod(klockan(5),10)+.01*klockan(6))))), disp(' '))

if exist('FIG')==1
    try
        close(FIG)
        pause(0.2)
    end
end

home
clear all
% wave_and_coeff.m calculates variables for this workspace

load string_prop.mat % BB23 T23 rho23
load sample_info.mat % T N dt Fs
t = linspace(0,T,N);
load wave_coeff.mat om freq L x_ex E23 diam23 mu23

ES23 = E23*pi*(diam23/2)^2; % The term E*S (Young's * cross sec area)
c_L = sqrt(E23/rho23); % Speed of sound of longitudinal waves
n_max = floor(2*L*freq(end)/c_L);
f_L = [1:n_max]*c_L/2/L;
tau_L = [1:n_max]*0.1;

load Long_displacement.mat % L_disp[n_max by length(t) Matrix]
load trans_disp_bridge.mat % Xi_IR_bridge xline_bridge str_resolut
% (Last 3 transversal values near the bridge and string resolution)
```



```
L_disp = L_disp(:,1:N);
L_disp_bridge = zeros(3,length(L_disp));

for gg=1:n_max,
    L_disp_bridge = L_disp_bridge + ...
        sin(gg*pi*xline_bridge'/L)*L_disp(gg,:);
end

F_Long = -[real(T23)*ones(1,length(L_disp)) + ...
    ES23*((-3*L_disp_bridge(3,:) + 4*L_disp_bridge(2,:) - ...
    L_disp_bridge(1,:))/(2*L/str_resolut)) + ...
    1/2*ES23*((-3*Xi_IR_bridge(3,:) + 4*Xi_IR_bridge(2,:) - ...
    Xi_IR_bridge(1,:))/(2*L/str_resolut)).^2];

save Longitudinal_Force.mat F_Long f_L % Longi force at bridge and the
% resonant frequencies of the longitudinal waves
```

Notations

Capital Letters

B	Bending Stiffness
E	Young's Modulus
F	Force
L	String Length
M_z	Moment about the z-axis
$O(\Delta x)$	Terms Of-Order-Of
S	Surface Area
T	Tension

Lowercase Letters

c	Wave Velocity
d	String Diameter
f	Frequency
j	$\sqrt{-1}$
k	Wavenumber
m	Mass
n	Modal Index
s	Stiffness
t	Time
x, y, z	Dimensional Units

Greek Letters

β	Bending Angle
Δ_{end}	Length of Support-Beam
ϵ	Correction Term Length
η	Vertical Displacement
μ	Mass per Unit Length
ξ	Longitudinal Displacement
π	3.14159265358979323846264338327950288419716939937510582...
ρ	Density
τ	Damping Factor
ω	Frequency

Subscripts

A	Amplitude
$+$	Positive k or Positive Traveling Wave/Near-Field Coefficient
$-$	Negative k or Negative Traveling Wave/Near-Field Coefficient
j	Imaginary k or Denoting a Near-Field Coefficient
$excite$	At the Excitation Point
t	Transverse Wave
l	Longitudinal wave
n	Transverse Modal Index
k	Longitudinal Modal Index
δ	Impulse Response

Superscripts

$'$	Per Unit Length
$''$	Per Unit Area

